The Landfall of Hurricane Hugo in the Carolinas: Surface Wind Distribution

MARK D. POWELL, PETER P. DODGE AND MICHAEL L. BLACK

NOAA/AOML, Hurricane Research Division, Miami, Florida

(Manuscript received 4 September 1990, in final form 9 May 1991)

ABSTRACT

Hurricane Hugo struck Charleston, South Carolina, on 22 September 1989 as the most intense hurricane to affect the United States since Camille in 1969. The northeastern eyewall, which contained the maximum winds measured by reconnaissance aircraft shortly before landfall, moved inland over a relatively unpopulated area and there were few fatalities. However, no observations were available to document the surface wind distribution in this part of the storm as it continued inland.

To improve specification of surface winds in Hugo, empirically adjusted aircraft winds were combined with coastal, offshore, and inland surface observations and were input to the Ooyama objective analysis algorithm. The wind analysis at landfall was then compared with subsequent analyses at 3 and 6 h after landfall. Reconstruction of the surface wind field at landfall suggests that the maximum (~13 min mean) surface wind at the coast was 50 m s^{-1} in the Bulls Bay region, ~40 km northeast of Charleston. Surface roughness over land caused wind speeds to drop off rapidly just inland of the coast to only 50% of values measured by reconnaissance aircraft at the same location relative to the storm over water. Despite relatively rapid increases in the central sea-level pressure and decreases in the mean circulation as Hugo progressed inland, hurricane-force wind gusts extended Hugo's damage pattern well past Charlotte, North Carolina, ~330 km inland.

Accurate determination of surface wind distribution in land-falling hurricanes is dependent upon the spatial density and quality of surface wind measurements and techniques to adjust reconnaissance flight-level winds to the surface. Improvements should allow forecasters to prepare more-accurate warnings and advisories and allow more-thorough documentation of poststorm effects. Empirical adjustments to reconnaissance aircraft measurements may replace surface data voids if the vertical profile of the horizontal wind is known. Expanded use of the airborne stepped-frequency microwave radiometer for remote sensing of ocean surface winds could fill data voids without relying upon empirical methods or models. A larger network of offshore, coastal, and inland surface platforms at standard (10-m) elevations with improved sampling strategies is envisioned for better resolution of hurricane wind fields. A rapid-response automatic station network, deployed at prearranged coastal locations by local universities with meteorology and/or wind engineering programs, could further supplement the fixed platform network and avoid the logistical problems posed by sending outside teams into threatened areas.

1. Introduction

When a hurricane warning is issued, preparations are initiated over an average of 550 km of coastline. These preparations have been estimated (Sheets 1990) to average $50 million per episode. The size of the warning area is dictated by: 1) uncertainty in the track and intensity forecast; 2) evacuation lead time for the threatened area; and 3) uncertainty in the surface wind distribution.

We do not know which factor is the most important determinant of the size of the hurricane warning area. Track forecast accuracy has gradually improved ~0.5% per year over the past 35 years (Sheets 1990) and has potential for more rapid improvements. Unfortunately, environmentally fragile coastal areas continue to be overdeveloped and are very popular for recreation. As a result, long evacuation lead times may be needed. According to the National Plan for Tropical Cyclone Research (OFCM 1990), the most pressing forecast and warning problem after track prediction is the specification of the surface wind distribution. The maximum sustained surface wind speed and the extent of hurricane- and tropical-storm-force winds at the surface are based upon reconnaissance aircraft measurements, rare surface observations from ships, or buoys and pressure/wind relationships. The National Hurricane Center (NHC) has only limited capability for incorporating the various available surface and flight-level observations into an analysis with a scale suitable for issuing advisories.

Recent improvements in objective analysis, airborne remote sensing of surface winds, and future surface observation networks have made it possible to devise an analysis system capable of synthesizing surface data from many types of platforms. This paper is a by-product of initial efforts toward devising such a system.

Corresponding author address: Dr. Mark Powell, Environmental Research Division/AOML, 4310 Rickenbacker Causeway, Miami, FL 33149.

Hurricane Hugo, the most destructive storm to make landfall since Camille in 1969, presented an opportunity to incorporate the Ooyama (1987) objective analysis algorithm into a surface wind analysis system. As analyses proceeded, we became aware of the potential application of the technique to real-time monitoring of the surface wind distribution for use in advisories and for determination of warning areas.

By 1800 UTC on 19 September 1989, Hurricane Hugo had weakened considerably from its passage over northeast Puerto Rico to a minimum sea-level central pressure (MSLP) of 966 mb and maximum sustained (1-min average) surface winds (V_{MSS}) estimated at 46 m s^{-1}. A gradual strengthening occurred as Hugo approached South Carolina over the next 48 h to MSLP of 944 mb and V_{MSS} of $\sim$54 m s^{-1}. During this period, Hugo's motion was influenced by two major synoptic flow features. As discussed by Case and Mayfield (1990) and indicated in Fig. 1, a cutoff low over the Florida Panhandle and the subtropical Atlantic ridge centered near Bermuda provided a deep layer of southeasterly flow that influenced the motion of the storm. An approaching midlatitude trough over the Rockies (mlt in Fig. 1) affected the acceleration of Hugo 24 h later. At 1800 UTC on 21 September, 10 h before landfall, Hugo began a period of rapid intensification to an MSLP of 934 mb and V_{MSS} estimated at 60.5 m s^{-1} by NHC. This intensification was consistent with a weakened environmental wind shear (personal communication, Mark DeMaria and Sim Aberson 1989) and passage over the Gulf Stream (Powell and Black 1990a). The detailed track of Hurricane Hugo's wind center, based upon aircraft fixes before landfall and surface wind observations after landfall, is shown in Fig. 2.

2. The wind field at flight level before landfall

When a well-established hurricane such as Hugo approaches land, ship data are usually only available on the storm periphery and, although helpful, the moored buoy network is of insufficient density to resolve the surface wind field. Often, the only direct measurements of hurricane wind distribution come from reconnaissance aircraft operated by the U.S. Air Force or NOAA at flight altitudes ranging from 500–3000 m, depending upon storm intensity. Since most of our current knowledge of hurricane wind fields is a result of analysis of flight-level observations from research or reconnaissance aircraft, we preface discussion of the surface

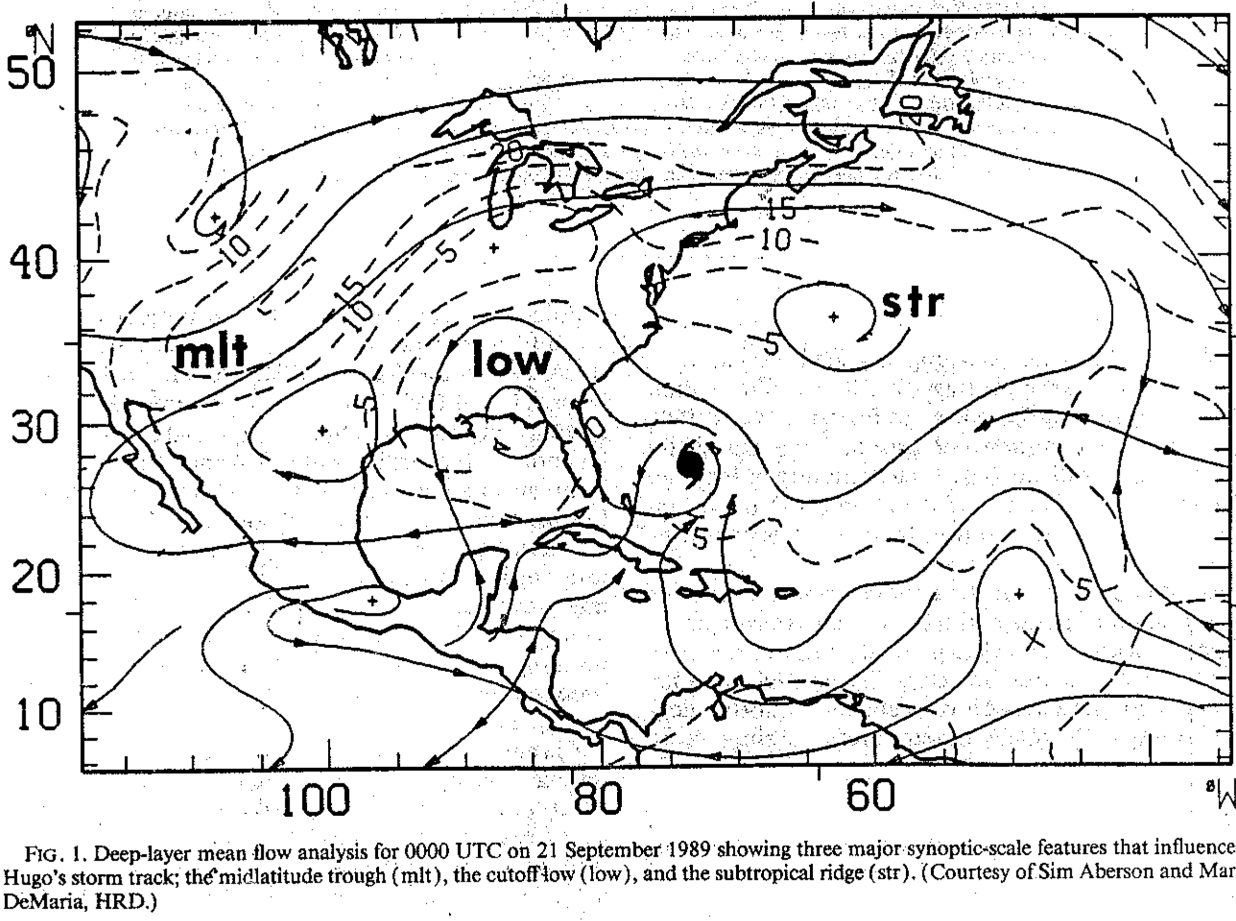

FIG. 1. Deep-layer mean flow analysis for 0000 UTC on 21 September 1989 showing three major synoptic-scale features that influenced Hugo's storm track; the midlatitude trough (mlt), the cutoff low (low), and the subtropical ridge (str). (Courtesy of Sim Aberson and Mark DeMaria, HRD.)

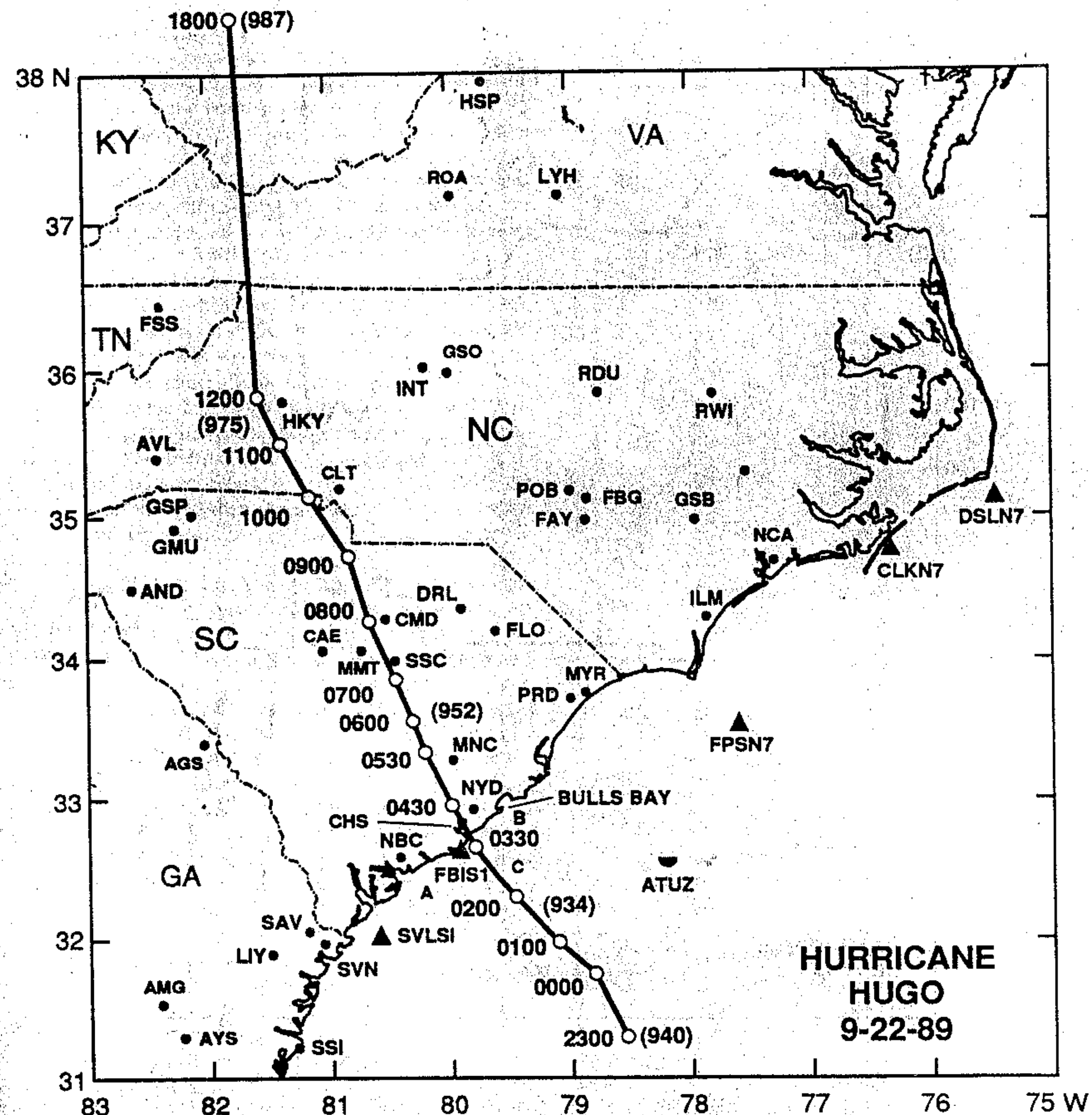

FIG. 2. Detailed track of Hugo's wind center. Surface observation sites are indicated by NWS, FAA, or NDBC call letters. Airborne Doppler radar wind profile locations are indicated by A (0120 UTC), B (0110 UTC), and C (0330 UTC).

wind distribution at landfall with a description of the wind field at flight level.

Before and during landfall, NHC relies on reconnaissance aircraft to report observations of the location, strength, and intensity of the storm. These data are transmitted to NHC in real time in the form of "vortex messages," which also supply the maximum wind speed observed during a particular transit through the storm. These values, shown plotted in Fig. 3, influence the estimated V_{MSS} mentioned in the public advisories. NOAA and most U.S. Air Force reconnaissance aircraft are also capable of sending high-resolution wind and thermodynamic data via aircraft–satellite data links (ASDL). Thus, NHC is provided with high-quality data at typical reconnaissance altitudes of 1.5–3 km. Because of safety considerations, Hugo was monitored at the 3.6-km level by a NOAA P-3 research aircraft for 6 h before landfall. The data collected by the aircraft consist of 1-min means sampled at a 1-min rate and provide the highest spatial and temporal resolution available

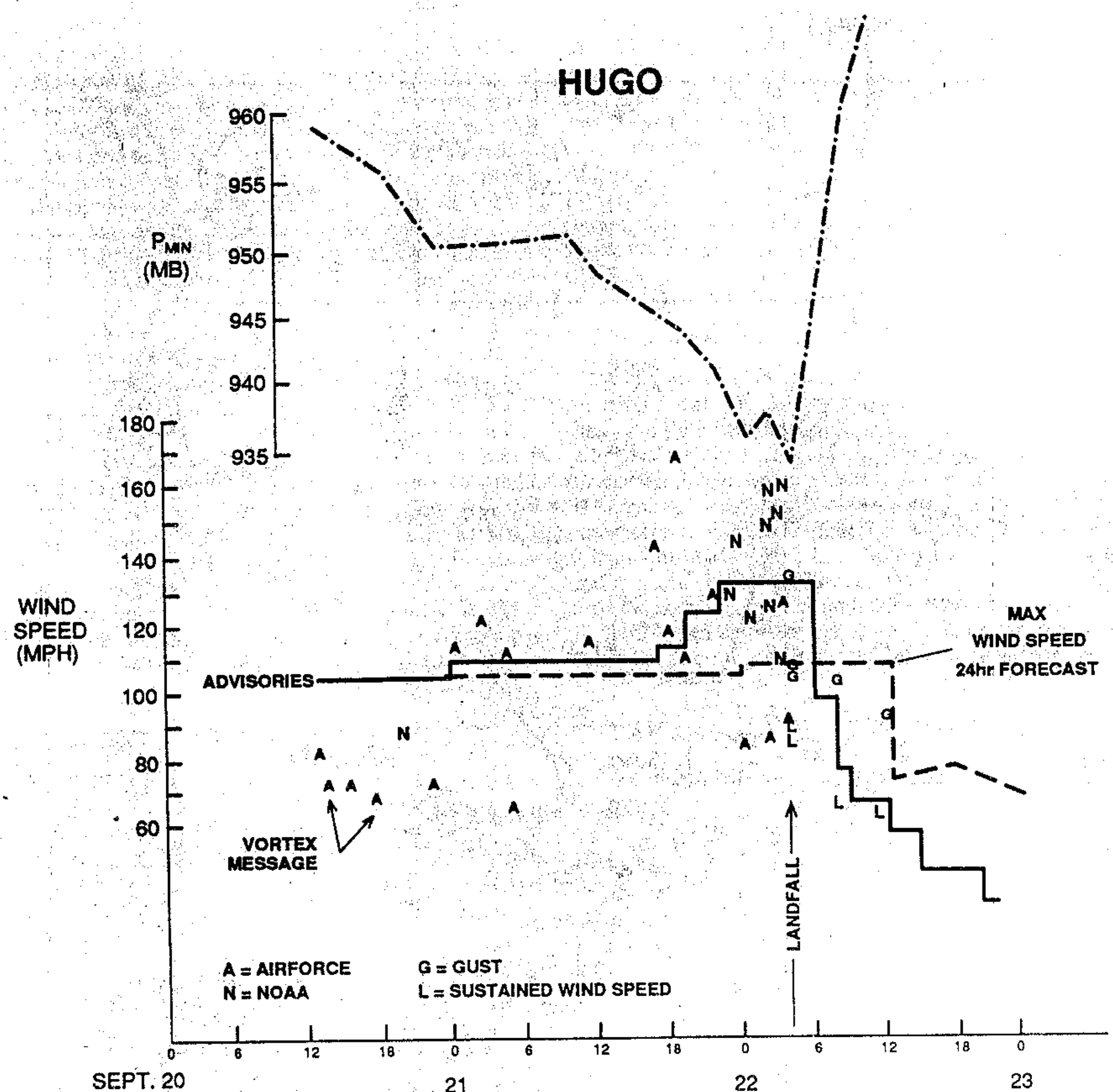

FIG. 3. Time (UTC) series of minimum central sea-level pressure (P_{MIN}), maximum flight-level wind speeds reported by NOAA (N) or U.S. Air Force (A) reconnaissance aircraft, maximum sustained surface wind estimates from the public advisories (solid line), and the 24-h forecast of this quantity (dashed line) verifying at the time labeled on the abscissa. Peak sustained (L) and gust (G) wind speeds measured at landfall are also shown.

for determining the wind field. Since these data are used to supplement the surface observations in data-poor regions, it is important to know the horizontal and vertical wind distribution at typical reconnaissance flight levels.

a. Method and analysis

In the storm-relative coordinate system chosen for the analyses, all observation locations over the time window of an analysis were transformed to a position relative to the storm center. The advantages of compositing data in a storm-relative system are discussed in Powell (1982, 1987). After transformation to the storm-relative coordinates, the input data were supplemented by the addition of locations in a 12.5-km radial and 15° azimuthal grid. Data were interpolated through a Barnes scan analysis. The basic wind analysis method is a mechanical interpolation technique (Ooyama 1987), which uses a two-dimensional (2D) least-squares fitting algorithm with a derivative constraint term. This acts as a low-pass filter on the analyzed field. Observational noise may be removed by the filter while features of the scale resolved by the data are retained. As implemented by Lord and Franklin (1987), the wind field is represented continuously throughout the analysis domain as a bilinear combination of basis functions (local cubic splines). These functions are twice-differentiable, allowing calculations of derived quantities without finite differencing.

Both flight-level and surface winds were analyzed on a 444-km × 444-km domain centered on the storm. A filter wavelength of 40 km was chosen to allow resolution of mesoscale wind features (eyewall and rainband wind maxima). This filter choice removes observational noise associated with exposure and sampling differences, including wind features that are too small (e.g., turbulent and convective gusts and lulls) to be adequately resolved by the observations. Analysis quality is monitored through deviation plots (between the input observations and the analysis) and divergence analyses.

Analysis of the NOAA aircraft wind measurements sent over the ASDL system from 2200–0400 UTC on 21–22 September in a storm-relative coordinate system is shown in Fig. 4. The coastline has been superimposed for the time of landfall. Note that the maximum winds observed by the aircraft were above the Bulls Bay area, ~40 km northeast of Charleston. The reflectivity distribution (Fig. 5), as measured by the LF (lower fuselage) radar aboard the P-3 shortly before landfall, indicates that the maximum winds were associated with the eyewall. Within the 65-m s^{-1} contour were the maximum measured winds of 71.5 m s^{-1}, which were not quite resolved by the chosen filtering wavelength. Strong winds > 35 m s^{-1} extend far to the north and east of the center, but weakened rapidly with radial distance on the south and west sides. This asymmetry was consistent with the storm motion of 12 m s^{-1} toward the northwest and a southeasterly background flow associated with the subtropical ridge (str in Fig. 1). These features would tend to reinforce flow on the northeast side of the storm and weaken flow on the southwest side.

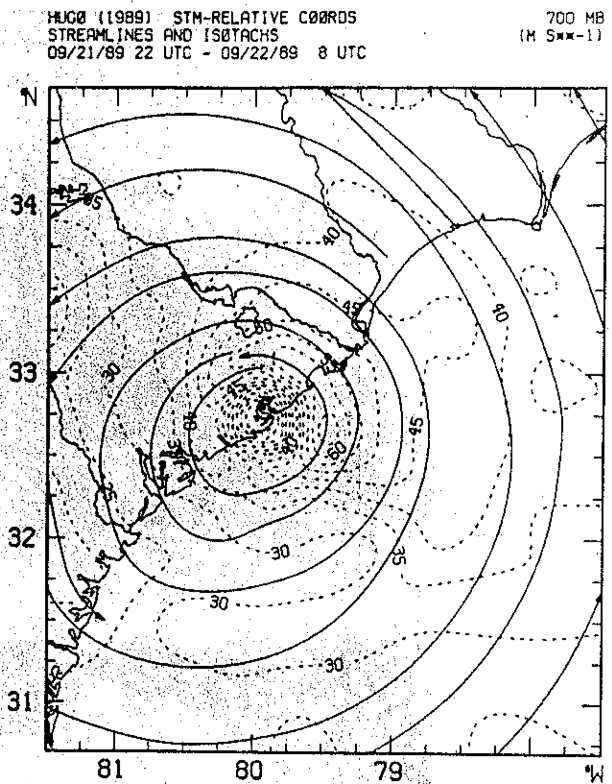

FIG. 4. Streamline and isotach objective analysis of NOAA aircraft winds measured at 3.6 km from 2200 UTC on 21 September to 0400 UTC on 22 September 1989 in a storm-relative coordinate system. Geography is indicated corresponding to storm position at 0400 UTC on 22 September 1989. Wind speeds are in m s^{-1}.

b. Vertical profile of the horizontal wind

Accurate estimation of surface wind speeds from reconnaissance flight-level wind measurements requires assessment of the level of maximum wind speed. Very little is known about the variability of the maximum wind level in the vertical profile of horizontal winds in hurricanes. Occasional rawindsonde information over land, multiaircraft research experiments, and recent airborne Doppler radar data collected over water by HRD suggest that a hurricane's maximum winds are usually found between 500 and 2000 m. The profile shape and height of the wind maximum may be dependent upon radius and quadrant and may also vary with proximity to land and convective rainbands.

Examples of horizontal wind profiles over land and water for Hurricane Hugo are shown in Fig. 6. The 0000 UTC rawinsonde launch from Charleston (CHS) was made when Hugo was only 170 km offshore, about 4 h before landfall. In this case, land friction has decreased winds near the surface, producing very strong wind shear from the surface to the maximum wind level of 2 km. Additional profiles in Fig. 6 were constructed from airborne Doppler radar wind measurements collected during near-orthogonal flight legs at 0120, 0110, and 0330 UTC for locations indicated as A, B, and C, respectively, in Fig. 2. Doppler radial velocity data were analyzed by the "pseudo dual-Doppler" technique (Jorgensen et al. 1983) over 10-km × 10-km analysis boxes and mean winds were computed for each horizontal level every 500 m in the vertical from 0.5 to 12.5 km. Unfortunately, the relatively high altitude of the aircraft (3.6 km) was such that the sampling volume of the beam was rather broad (300–600-m vertical depth of beam) at low levels, so detailed boundary layer wind structure could not be resolved.

Profiles A and B were on each side of Charleston. Profile A was ~28 km offshore from Edisto Beach at

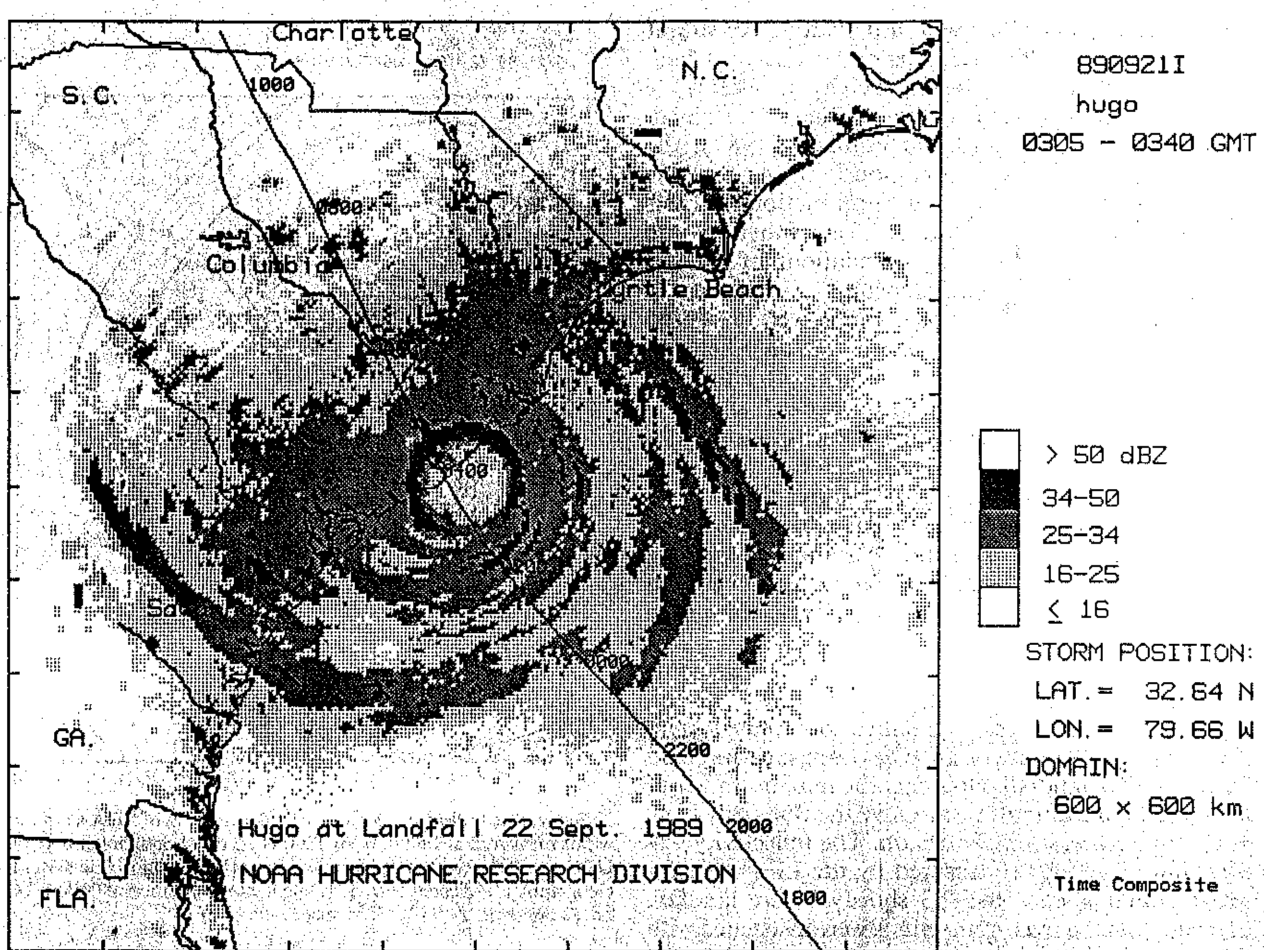

FIG. 5. Storm-relative composite of NOAA P-3 lower fuselage radar reflectivity distribution from 0305–0340 UTC for 22 September 1989. Geography is positioned for 0400 UTC according to wind center track from Fig. 1.

2 h 40 min before landfall, and B was ~35 km offshore from Bulls Bay at 2 h 50 min before landfall. Both A and B were in stratiform rain areas on the outer side (side farthest from the eye) of the first prominent rainband outside the eyewall. Wind maxima for A and B are at 1500 and 500 m, respectively. Because of broad Doppler radar beam volumes, there is insufficient resolution to show the decrease in wind speed as the surface is approached. Neither profile shows the strong shear pattern indicated over land. The decrease of wind speed with height above 1.5 km is consistent with weakening of the horizontal pressure gradient with height, typical of warm-core cyclones.

Profile C was measured in the southeast quadrant of the eyewall shortly before landfall, while the northwest quadrant of the eyewall was crossing the coast at Folly Island. This profile indicates maximum winds at 1 km with very little shear through the 8-km level. Multiple-level aircraft observations in other hurricanes (e.g., Jorgensen 1984) have indicated considerable shear with an outward tilt of the maximum eyewall winds on the inner side of the eyewall radar reflectivity maximum. Such a tilt could show a low-level maximum at an inner radius and an upper-level maximum at a larger radius. Outward tilt was not obvious in the Hugo Doppler analysis. The lack of shear in Hugo's eyewall may have been caused by the vertical transfer of horizontal momentum by intense convection. Hourly surface observations (0000–0300 UTC) at the Folly Island Coastal Marine Automated Network (CMAN) station (FBIS1) are included as filled triangles in Fig. 8 for comparison. These observations were made in partial over-water flow in a storm-relative location between profiles A and B. The coastal boundary layer vertical shear may be estimated by connecting profile A with surface point 0 or 1 (3×10^{-2} s^{-1}), connecting B with 2 (4×10^{-2} s^{-1}), and connecting C with 3 (3×10^{-2} s^{-1}).

The above profiles illustrate a common data interpretation problem facing hurricane forecasters in a potential landfall situation; that is, the strongest winds in the hurricane may not be sampled by the reconnais-

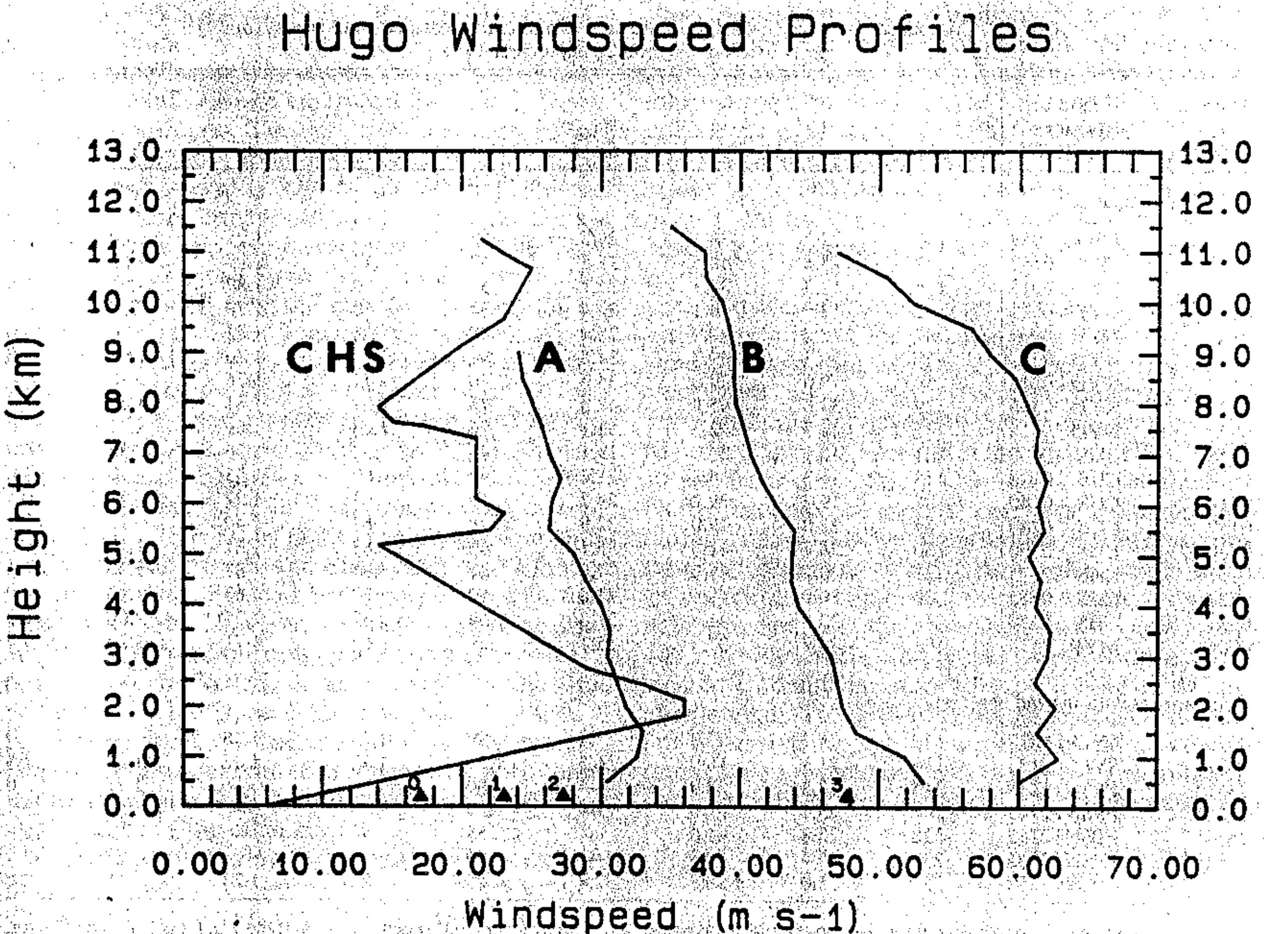

FIG. 6. Vertical profiles of the horizontal wind. The 0000 UTC on 22 September 1989 rawinsonde launch at Charleston, South Carolina, is at far left. Airborne Doppler radar analysis box profiles are designated as: A at 0120 UTC; B at 0110 UTC; and C at 0330 UTC in locations shown in Fig. 1. Triangles indicate surface wind measurements from FBIS1 at 0000 (0), 0100 (01), 0200 (02), and 0300 (03) UTC.

sance aircraft. Remote measurements by stepped frequency microwave radiometer (SFMR) (Black and Swift 1984) have a good chance of solving this problem, but only one instrument is currently installed on a NOAA aircraft. If the aircraft is near the maximum wind level and at <1500 m, marine planetary boundary layer (PBL) models may be used to determine a reasonable estimate of the surface wind speed (Powell 1980). If the aircraft is above these levels, as it was in Hugo, surface winds can be estimated from empirical relationships (Powell and Black 1990b). Much further analysis of wind profiles is required to determine how the vertical profile of the horizontal wind varies with radius, quadrant, and proximity to rainbands and land.

3. Comparisons of flight-level and surface wind measurements

As shown in Fig. 2, there were no observing sites in the region where the aircraft had measured maximum winds between the North Charleston Navy Yard (NYD) and Myrtle Beach Air Force Base (MYR). Lack of surface data in this region prevented observation of maximum winds in the southwest end of Bulls Bay. This area experienced the northeast eyewall of the hurricane, as shown in the radar display in Fig. 5. Below, we discuss how comparisons of aircraft and surface measurements were used to adjust aircraft observations to the surface and fill in data-sparse portions of the landfall wind analysis.

Until surface wind speed can be measured remotely by all reconnaissance aircraft, we must be able to estimate the V_{MSS} from aircraft measurements above the surface. Powell and Black (1990b) sought to estimate V_{MSS} from flight-level measurements by comparing aircraft and surface winds to obtain empirical adjustment ratios. They compared NOAA aircraft winds (30 s mean), V_A, with surface winds, V_B, measured over water by moored NOAA data buoys in the Atlantic and Gulf of Mexico for hurricanes from 1975–1987. Characteristics of the buoy platforms are described by Gilhousen (1987). Least-squares fits of V_B versus V_A

TABLE 1. Comparisons of surface platform-measured and aircraft-measured wind speeds (m s^{-1}) in Hurricane Hugo on 22 September 1989.

Aircraft time (UTC)	Surface platform time (UTC)	R (km)	V_S m s^{-1}	V_A m s^{-1}	V_{SG} m s^{-1}	V_S/V_A	V_{SG}/V_A	G	Δt	Δr
Overland comparisons										
0019	FBIS1 0059	108	22.2	35.7	26.8	.62	.75	1.21	−.67	6.2
0157	FBIS1 0159	57	27.6	48.5	35.2	.57	.73	1.27	−.03	16.2
0018	NYD 0115	114	11.3	35.5	21.1	.32	.59	1.87	−.95	1.5
0114	NYD 0145	92	13.5	39.1	23.4	.34	.60	1.73	−.52	6.0
0113	NYD 0200	87	15.4	40.9	28.0	.38	.68	1.82	−.70	4.0
0156	NYD 0300	50	20.3	49.7	34.6	.41	.70	1.70	−1.06	1.0
0157	NYD 0245	54	19.6	29.0	34.6	.40	.71	1.76	−.80	9.0
0329	NYD 0500	29	34.6	45.5	48.8	.76	1.07	1.41	−1.50	5.0
0330	NYD 0515	37	32.3	42.3	52.1	.76	1.23	1.61	−1.75	2.0
0018	CUS 0040	121	15.1	36.5	19.1	.41	.52	1.26	−.36	16.0
0019	CUS 0100	113	16.3	35.8	21.6	.45	.60	1.33	−.70	3.0
0114	CUS 0140	88	19.4	39.2	24.7	.50	.63	1.27	−.43	0.5
0157	CUS 0240	51	22.0	49.0	32.9	.45	.67	1.49	−.72	2.0
0330	CUS 0500	36	26.7	42.3	35.1	.63	.83	1.31	−1.50	0.5
0157	CHS 0315	48	20.2	49.0	27.8	.41	.57	1.37	−1.30	2.0
0327	CHS 0515	30	25.0	48.1	41.8	.52	.87	1.67	−1.80	4.0
0331	CHS 0530	44	22.3	41.4	27.8	.54	.67	1.25	−2.00	1.0
0004	MYR 0115	192	14.7	37.3	25.1	.39	.67	1.71	−1.20	1.0
Comparisons with marine observations										
0030	SVLS1 0059	138	21.7	22.0	27.4	.99	1.25	1.26	−.48	2.3
0042	SVLS1 0159	116	21.8	18.0	26.5	1.21	1.47	1.22	−1.28	1.1
2357*	FPSN7 2235	245	23.3	38.9	—	.60	—	—	1.36	1.0
2355*	FPSN7 2245	244	23.1	39.0	—	.59	—	—	1.17	3.7
2354*	FPSN7 2255	238	23.8	41.0	—	.58	—	—	.98	1.8
2353*	FPSN7 2305	230	23.4	33.5	—	.70	—	—	.70	11.9
2356	FPSN7 2259	251	25.0	38.5	30.8	.65	.80	1.23	.65	4.6

R = radial distance from storm center, V_S = overland wind speed, V_A = flight-level wind speed, V_{SG} = surface wind gust, G = gust factor, Δt = aircraft time − surface ob time, Δr = radial separation.

* From consecutive 10-min average.

showed high correlation with slopes (ratio V_B/V_A) varying from 0.6 in stable surface layer conditions to 0.8 in unstable conditions, with a 0.15 standard deviation. Typical gusts (5–8 s average) measured by the buoys were 30% higher than V_B. Hence, a V_B of 35 m s^{-1} would likely contain a peak gust of 45 m s^{-1}.

In Hugo, the aircraft and surface platforms were compared in a storm-relative coordinate system. Comparisons (Table 1) were made only when radial separations were <15 km and time separations were <2 h. Over land, there were 18 comparisons from 5 platforms, which included 8 comparisons near the eyewall (between 30 and 50 km from the center). Over water, there were only six comparisons from two platforms. Platform locations are indicated by a 3-letter code (overland) or a 4–5 letter code for coastal and offshore stations in Fig. 2. Table 2 lists platform averaging times and anemometer heights.

Overland comparison locations include the FBIS1 and the NWS anemometer at the Charleston Customs House (CUS). Upwind fetches at these sites were partially over water before landfall. Other sites included NYD, CHS, and MYR, which are all assumed to have open exposures. Overwater comparisons that fit the time and space criteria could be made only for the

TABLE 2. Surface platform observation characteristics.

Platform	Anemometer height (m)	Averaging period (min)	Exposures
Folly Island CMAN (FBIS1)	10.0	2	Land, water
North Charleston Navy Yard (NYD)	36.0	15	Land
Charleston Customs House (CUS)	7.6	1	Land, water
Charleston NWS Airport (CHS)	6.7	10	Open land
Myrtle Beach AFB (MYR)	4.6	15	Open land
Savannah CMAN (SVSL1)	32.6	2	Water
Frying Pan Shoals CMAN (FPSN7)	43.5	2, 10	Water

Savannah (SVLS1) and Frying Pan Shoals (FPSN7) CMAN stations.

All comparisons of overland surface observations near the eyewall were <5 km from the aircraft in storm-relative coordinates. The surface winds were 56% of the mean flight-level wind on the average, and the peak surface gusts averaged 82% of the mean flight-level winds. Including noneyewall comparisons, the average was 49%, with peak gusts averaging 72% of the flight-level mean. The gust factor (ratio of the surface gust to the mean wind over the sampling period) for the overland sites in Table 1 averaged 1.5. Comparisons during the landfalls of Hurricanes Frederic (1979) and Alicia (1983) on the Gulf of Mexico coastline (Powell 1982, 1987) are summarized in Table 3. The ratio of surface to aircraft mean winds (V_S/V_A) in Frederic and Alicia was about 60% as compared with 49% in Hugo, and peak gusts in these storms were a larger percentage of the mean flight-level winds. The comparison sets for Frederic and Alicia comprised a limited amount of data that had less-stringent criteria than those used above. However, a Student's t test (Panofsky and Brier 1965) of the null hypothesis that the V_S/V_A ratio samples in Frederic or Alicia were from the same population as the Hugo ratios was rejected at the 5% significance level. The significantly smaller ratios in Hugo are consistent with the influence of more dense-terrain roughness features (large areas of forest) than were evident in the other storms.

Over water, the comparisons with SVLS1 are very unusual, showing surface measurements greater than the aircraft despite offshore flow. A reason for high ratios at SVLS1 might be mixing of stronger (than flight-level) winds from near the 500–1800-m height because of unstable stratification (cool air over warm water). At FPSN7, no sea surface temperatures were available, but cooler temperatures were suggested by a poststorm analysis (Powell and Black 1990a). The ratios here, which were only 60%–65% of flight-level values, are consistent with more-stable boundary layer stratification.

4. Determination of the surface wind distribution at landfall

The actual maximum sustained surface winds experienced at landfall are unknown, since no surface wind measurements were available in the part of the storm where reconnaissance aircraft had measured peak wind speeds just before landfall. Based upon the information available from the reconnaissance aircraft and other methods (Sheets 1990), advisories issued by NHC estimated V_{MSS} of 60.5 m s^{-1} (85% of the maximum V_{FL}). The highest V_{MSS} actually measured was 39 m s^{-1} at the NWS automatic station at CUS. The highest (1-s) gust in Hugo was 61.4 m s^{-1}, measured at NYD.

Unfortunately, surface observing sites were not optimally positioned for recording the region of peak winds in the northeast part of the eyewall. Hurricane chase teams documented eyewall and rainband reflectivity structure for several hours with portable radar recorders that were operated at the NWS WSR-57 radar sites at Charleston, South Carolina, and Wilmington, North Carolina. The evolution of the precipitation field during landfall is shown in the sequence of sweeps from the Charleston radar in Fig. 7. Although there was some ground clutter contamination in the Charleston radar data, it is clear that the eyewall affected an area about 100 km wide, with some indication that the eye decreased in diameter from 55 km offshore to 45 km after landfall. The eyewall appeared to thicken at landfall; this change was probably caused by enhanced frictional inflow over land, which allowed precipitation particles to be advected closer to the storm center.

a. *Surface wind measurements in Hugo*

At landfall, power outages, damaged sensors, communication problems, and infrequent interrogation methods usually prevent forecasters from assessing the surface wind field in real time. With implementation of an objective analysis technique and adoption of the recommendations mentioned in the conclusions and appendix, near-real-time analyses combining aircraft-adjusted, land surface, and oceanic platforms could become a standard product available to forecasters. If observations are composited relative to the storm center over a period of several hours when the intensity change is minimal, data voids could be filled and surface streamline/isotach analyses could be produced as discussed below.

Despite Hugo's severity, enough anemometer records survived to allow reconstruction of the surface

TABLE 3. Mean ratios of surface mean wind and gust to flight-level mean and mean surface gust factors from comparisons of surface and aircraft data in landfalling hurricanes.

Storm	Year	Number of comparisons	V_S/V_A	(σ)	V_{SG}/V_A	(σ)	G	(σ)
Frederic	1979	10	.58	(.10)	.80	(.11)	1.39	(.15)
Alicia	1983	13	.59	(.14)	.95	(.21)	1.64	(.27)
Hugo	1989	18	.49	(.13)	.73	(.18)	1.50	(.23)

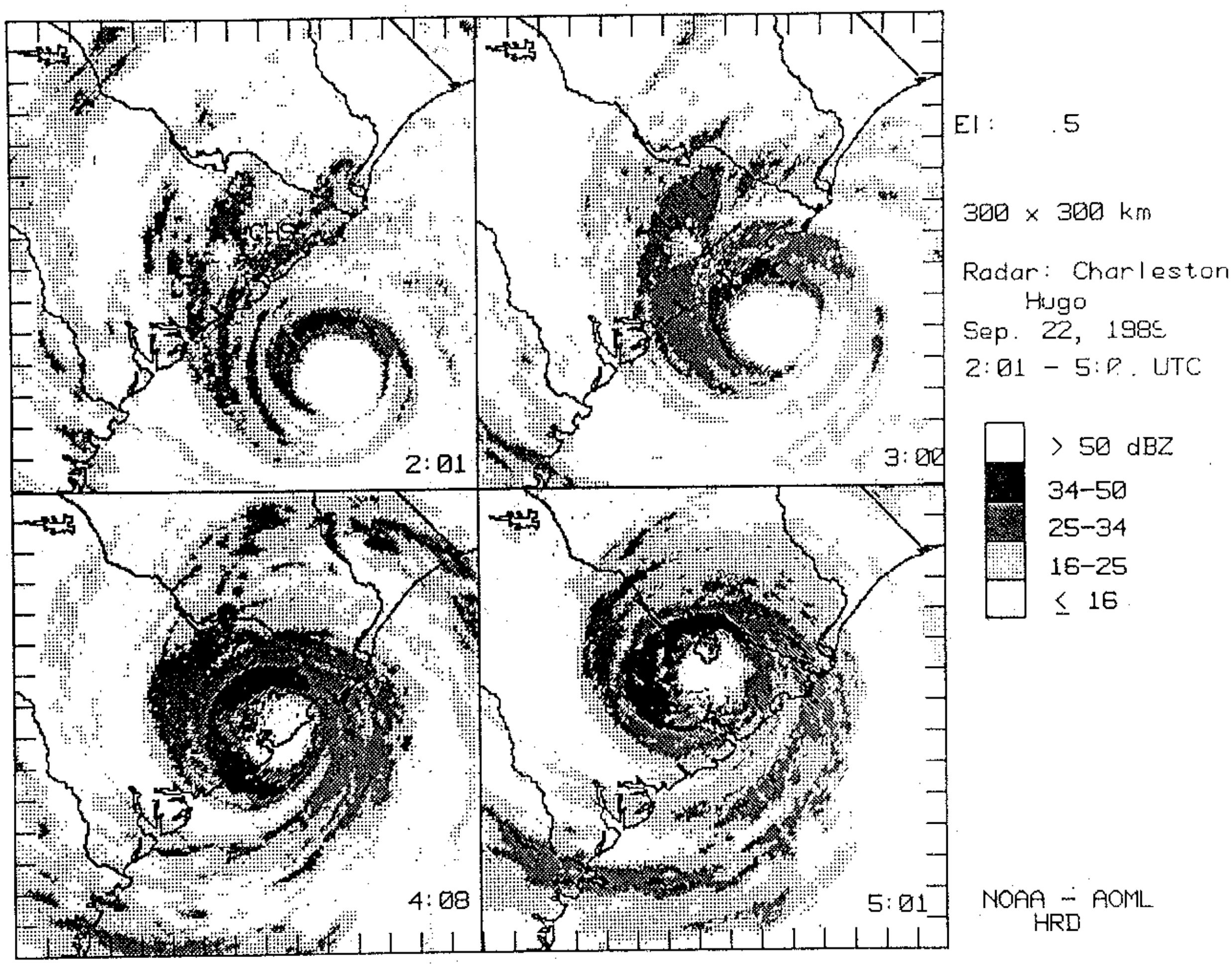

FIG. 7. Sequence of sweeps from digitized land-based radar observations recorded from the Charleston NWS WSR-57 radar for (a) 0201, (b) 0300, (c) 0408, and (d) 0501. All times in UTC on 22 September 1989.

wind field. Ideally, analysis of surface data would require that these observations be collected in a standard, consistent manner. The distribution of surface observation sites relative to the storm track is evident from Fig. 2. Unfortunately, these sites comprise anemometer heights ranging from 4–44 m, averaging times from 1–15 min, different types of instruments with different performance characteristics, and various upwind terrain exposures. As discussed in the appendix, no standardization methods were used to resolve sampling scale differences among observation platforms. Very few surface observations adhere to the World Meteorological Organization's (WMO) recommendation of a 10-m anemometer height; most NWS sites are at airports and use heights of 6 m. Fortunately, mean winds can be adjusted to 10 m, provided the terrain roughness upwind of the anemometer can be estimated. Here, a neutral stability log-law (Panofsky and Dutton 1984) was used to adjust all land anemometers to 10 m. Over water, we used an air–sea interaction boundary layer model (Liu et al. 1979) to adjust CMAN stations to 10 m.

b. Adjustments based on comparisons of aircraft and surface data

To fill in sparse areas of the storm-relative data distribution at landfall, the aircraft winds were adjusted to the 10-m level. Over land, an empirical adjustment of 60% was applied to the flight-level winds, since this was the mean reduction observed near Hugo's eyewall and was also the mean ratio for all comparisons in Frederic and Alicia (Table 3). Wind-direction backing of 36° was used over land to allow for greater friction, based upon comparisons of aircraft and surface wind directions. Over water, aircraft flight level was too high to properly apply a boundary-layer model adjustment to the winds. An empirical value of 76% was used, based upon buoy–aircraft comparisons (Powell and Black 1990b). Backing of 25° was used to account for surface inflow over the water.

c. *Surface wind field analysis at 0400 UTC*

A 2200–0600 UTC time window, 6 h before landfall to 2 h after landfall, was chosen for the landfall analysis. As indicated in Figs. 2 and 3, this period corresponded to a central pressure decrease from 940 (2200 UTC) to 934 mb (0400 UTC) followed by an estimated increase to 952 mb (0600 UTC). Although minimal storm intensity changes desired for composite analyses were not indicated by the pressure observations, the wind observations collected over this period are considered to be representative of a landfalling hurricane.

One storm-relative analysis was made using all land stations and land-adjusted aircraft winds during the time window. Another analysis was made using only oceanic platforms and ocean-adjusted aircraft data for the same period. Geography corresponding to the storm location at 0400 UTC was overlayed on each analysis and portions over inappropriate exposure locations were rejected (e.g., any part of the land station analysis located over the water after overlaying geography was removed). The two analyses were then manually joined at the coastline, resulting in a discontinuity where overwater flow changed to overland and vice versa. According to the sampling volumes for the range of input data averaging times (see appendix; Fig. 15), the spatial scales of wind features recorded by the observation platforms ranged from micro alpha scale (1 km) to meso gamma scale (20 km). After application of the 40-km filter wavelength, the resulting analyses were considered to be mesobeta scale with wind features comparable with what might be measured over a 13–20-min averaging period in greater-than-hurricane-force wind speeds. Because of computation platform constraints, this filter wavelength was the smallest allowed by the analysis algorithm for the domain of interest.

The resulting streamline and isotach analysis in Fig. 8 shows a highly asymmetric wind field with strong inflow on the southeast side of the storm and weaker inflow on the northwest side. The strongest winds in the analysis are found at the 50-m s^{-1} isotach 40 km northeast of Charleston at Bulls Bay. For the wind analysis to be applied in real time, the forecaster must be able to estimate the V_{MSS} required for the advisory. If we assume that the hurricane wind field is stationary for 13–20 min at the location of the maximum speed, and that the frequency distribution of wind speed is approximately Gaussian, the method of Durst (1960) (discussed in section 6) allows estimation of the highest 1-min mean speed over the period. Using the peak isotach contour of 50 m s^{-1}, with a filter wavelength of 40 km, Fig. 15 yields a sampling time of 13 min. Durst's method suggests a V_{MSS} 15% higher than the mean over this period, or 57.5 m s^{-1}. Powell and Black (1990b) suggest estimating surface winds by a 76% adjustment to the maximum flight-level winds, yielding a maximum (8.5 min mean) surface wind of 54 m s^{-1},

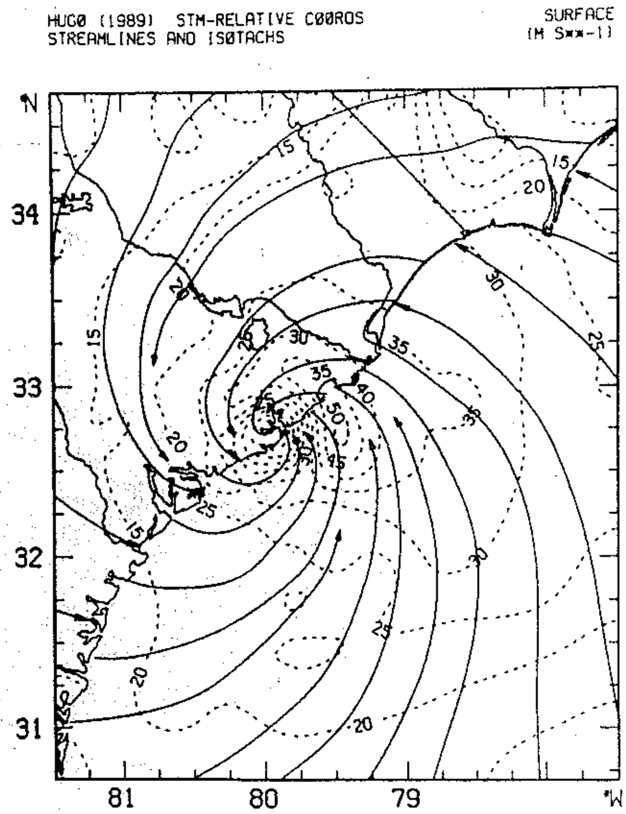

FIG. 8. As in Fig. 4, but for surface winds measured by oceanic, land-based, and adjusted aircraft platforms for 0400 UTC for 22 September 1989.

which converts to V_{MSS} of 59.8 m s^{-1}. These values are consistent with the V_{MSS} of 60.4 m s^{-1} used by NHC in the landfall advisories.

An important feature in the analysis is the discontinuity at the coastline, where the analyses were merged. Here, strong overwater winds abruptly weaken in onshore flow and frictionally reduced winds accelerate in offshore flow. Actually, this discontinuity is a transition zone where a new internal boundary layer forms as the flow adjusts to a new underlying surface. The height of the internal boundary layer (H_i) is a function of the aerodynamic roughness (Z_0) of the new terrain and fetch from the start of the roughness change. The length of this transition zone may be estimated by calculating the fetch required for the turbulent wind at anemometer level (10 m) to reach equilibrium with the new surface. If we use a fetch of 1 km and representative roughness estimates of Z_0 = 1 m for the forested terrain in the Bulls Bay area, and Z_0 = 1 cm over water to the southwest of the center, the formulation for H_i (Arya 1988) yields 95 m for Bulls Bay and 38 m for the region to the southwest of the center over water. According to Peterson (1969), however, in neutral stability conditions only the lower 10% of the new internal boundary layer is actually in equilibrium with the new surface. Hence, for onshore flow, a fetch of ~1 km over rough

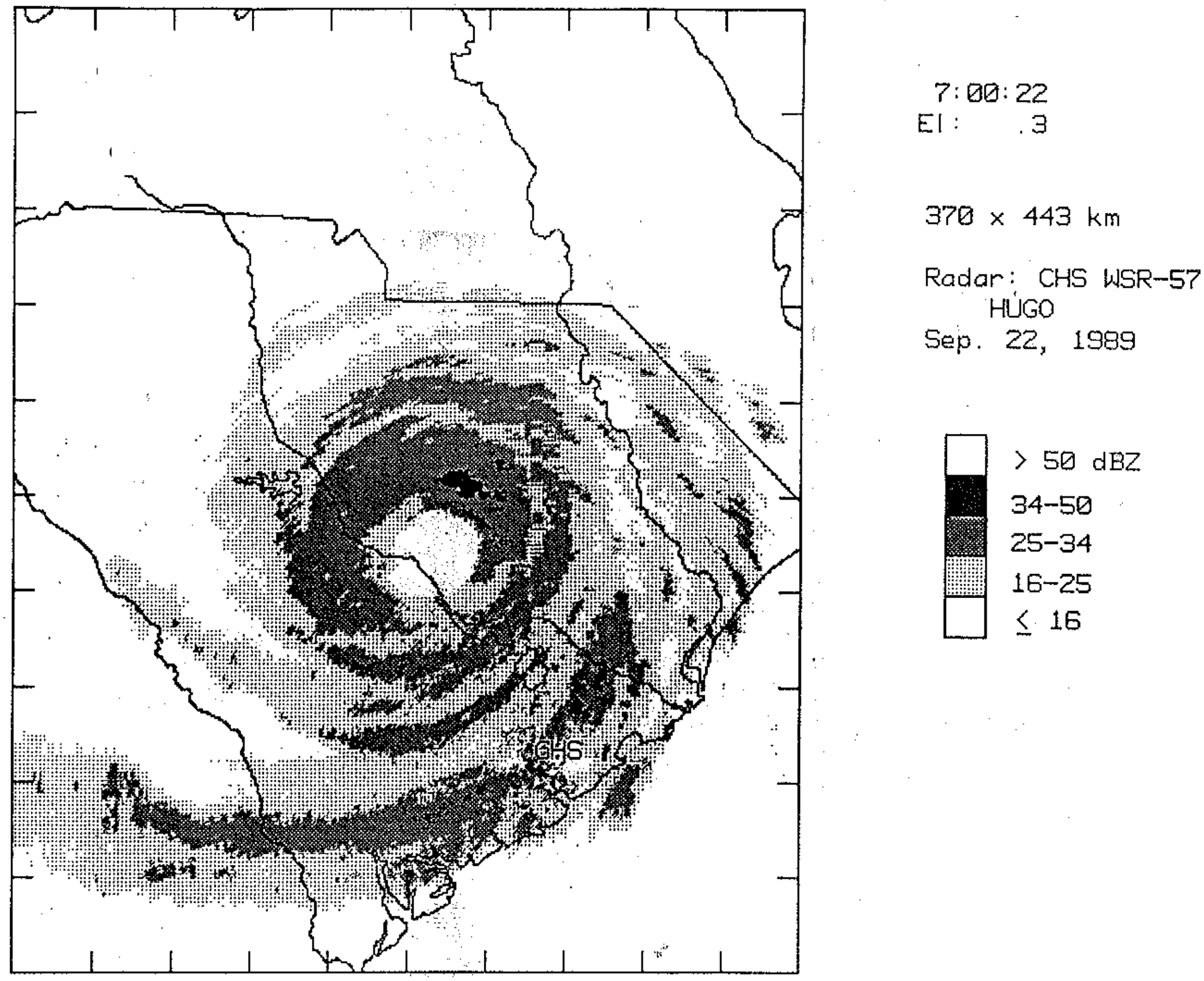

FIG. 9. As in Fig. 7, but for 0700 UTC on 22 September 1989 when Hugo was in the vicinity of Shaw Air Force Base.

terrain would be required for the 10-m level to be in equilibrium, while offshore flow to the southwest of the center would require a fetch of ~3.5 km. If conditions were more stable over rain-cooled land, a longer onshore fetch would be probable, while more unstable conditions over warm water might produce a shorter offshore fetch.

Similar coastal wind discontinuities were observed in Hurricanes Frederic and Alicia. An extreme example is given by SethuRaman (1979) for the landfall of Hurricane Belle (1976) on the south shore of Long Island. In this study, SethuRaman examined measurements from three anemometers that were oriented along a line perpendicular to the coast, at 10-km separation. During onshore flow over a 4-h period before landfall, the coastal winds were a factor of 2 greater than those 10 km inland and a factor of 4 greater than those measured 20 km inland.

d. Validation of public advisories

The onset of tropical-storm-force winds is a determining factor for the completion of emergency-preparedness activities. Based upon hourly surface reports, tropical-storm-force winds (>17.7 m s^{-1}) were first observed by the CMAN stations (2-min average at or adjusted to 10-m level), beginning at 1910 UTC on 21 September, for FPSN7 (311 km north-northeast of the center), at 2300 UTC for SVLS1 (255 km northwest of the center), and at 0000 UTC on 22 September at FBIS1 (178 km northwest of the center). At Charleston (CUS), tropical-storm-force winds were not experienced until 2 h 40 min before landfall at 0120 UTC, when the storm was 122 km offshore. Both SVLS1 and FPSN7 are well-exposed offshore sites, while FBIS1 is a well-exposed beach site with partial overwater exposure. CUS is a riverside site with good partial overwater exposure before center passage and poor exposure after. The distances for onset of tropical-storm-force winds at FPSN7 and SVLS1 are 20%–35% less than the radius of tropical-storm-force winds given in the marine advisories issued at 2200 UTC (403 km).

Based upon the analysis and inland surface measurements, sustained hurricane-force winds over land were not evident radially outward from the left side of the eyewall, but were found outside the front, rear, and right sides to a maximum distance of 75 km from the center. At the coast and over water, Fig. 8 and CMAN observations indicate hurricane-force winds 135 km to the right and rear, but not to the left of the center. Public advisories at this time warned that hurricane-force winds extended 225 km east of the center and up to 80 km to the west.

The lack of agreement on the extent of tropical-storm and hurricane-force winds between advisories and poststorm analyses is indicative of the uncertainties in the wind distribution, forecast track, and forecast intensity. Note that much of the input data for the analyses were unavailable to NHC in real time. Reports forwarded to NHC in real time over the amateur radio network were often unconfirmed and some proved to be inaccurate, based upon observed damage. For example, the vessel "Snowgoose," located 25 km upriver from Georgetown, about 80 km northeast of Charleston, reported sustained 54-m s^{-1} winds (Case and Mayfield 1990), which did not correlate with analysis winds of 20–25 m s^{-1} or with minimal damage to trees in the vicinity (personal communications: Marilyn Buford, Research Forester; Peter Sparks, Clemson University).

While near-real-time surface wind observations have little influence on forecasts, they are a very useful component in the preparation of warning and watch areas and as a nowcasting tool to keep the public informed in advisories. Therefore, it is important that the latest observations be available to the forecaster in a timely manner. Unfortunately, standard hourly observations, even when plotted in a storm-relative framework, do not have adequate time resolution to resolve the most important details of the wind field of a fast-moving hurricane. One contribution to more-accurate surface wind field specification would be the ability to call up more frequent or continuous observations. Such ability is a very desirable feature for automatic weather stations.

5. Surface wind fields as Hugo progressed inland

Hugo maintained enough of its circulation to do considerable wind damage well inland. The following analyses depict the wind fields associated with Hugo's passage (Fig. 2) through Columbia, South Carolina (CAE), at 0700 UTC and Charlotte, North Carolina (CLT), at 1000 UTC.

a. Surface wind analysis at 0700 UTC

As shown (Fig. 9) in the 0700 UTC sweep from the Charleston radar, Hugo's center was between CAE and Shaw Air Force Base (SSC), with SSC in the region of intense reflectivity on the northeast side of the eyewall. Surface observations for the 0700 UTC analysis were collected from 0500–0900 UTC. During this period, Hugo's MSLP was rapidly filling from near 940 mb at 0500 UTC to 961 mb at 0900 UTC. The resulting surface analysis (Fig. 10) is representative of a decaying hurricane and indicates that Hugo was just below hurricane strength, with mean winds near 30 m s^{-1} in the northern part of the eyewall. An outer secondary wind maxima > 20 m s^{-1} and 145 km to the northeast was associated with peak wind reports from Myrtle Beach (MYR) and Florence (FLO) in the early part of the analysis time window. Compared with the 0400 UTC analysis (Fig. 8), surface inflow increased in all but the southwest quadrants as the MSLP increased.

At 0800 UTC, advisories indicated V_{MSS} of 36 m s^{-1} with tropical-storm-force winds extending 160 km from the center. The extent of tropical-storm-force winds depicted by the analysis was 150 km and the V_{MSS} from the advisory was reasonable, considering the possibility

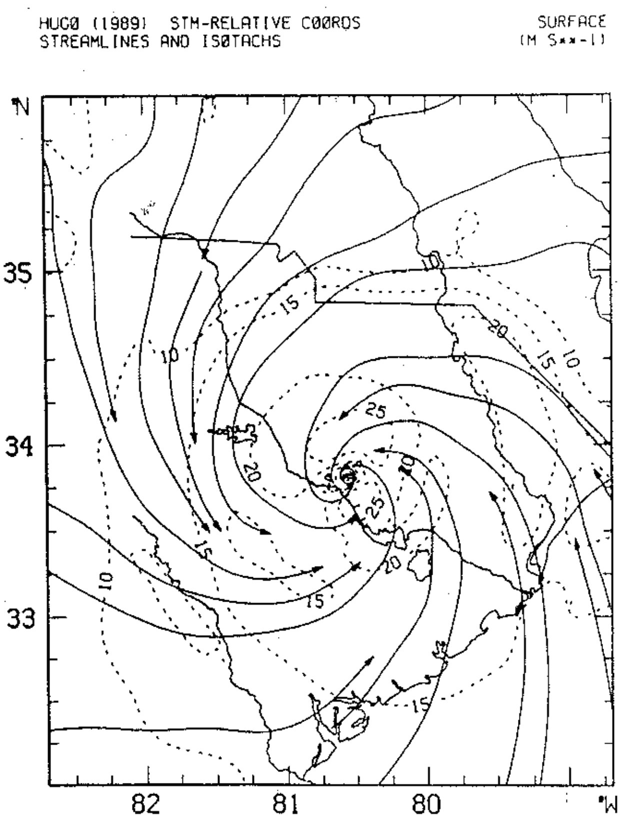

FIG. 10. As in Fig. 8, but for 0700 UTC on 22 September 1989. Data collection input is 0500–0900 UTC.

that SSC might have missed the V_{MSS} by a few kilometers. However, the intense radar reflectivities of up to 39 dBZ at 0630 UTC (Fig. 9) indicate that the strongest part of the eyewall passed over SSC.

A time series of radar reflectivity, 15-min mean winds, and peak gusts within each 15-min period for SSC (Fig. 11) illustrate the effect of convective rainband features on the wind. Wind maxima appear in the northeast eyewall at 0630, in the southeast eyewall at 0720, and in several outer rainbands afterwards in accordance with Fig. 10. The high correlation between gusts and reflectivity maxima is consistent with observations by Parrish et al. (1982), suggesting that peak gusts are caused by downdrafts in intense rainfall areas.

b. Surface wind analysis at 1000 UTC

By 1000 UTC, Hugo had continued on a north-northwest track to near CLT. By this time the remnants of the eyewall of Hugo could no longer be observed by the NWS radars at Charleston or Wilmington. The 0800–1200 UTC period was chosen for the 1000 UTC surface wind analysis. During this period, the MSLP increased from near 957 mb to 975 mb. Hugo was downgraded to a tropical storm in the 1000 UTC advisory, which mentioned V_{MSS} of 31 m s^{-1}. The 1000 UTC analysis (Fig. 12) indicates that maximum winds were reduced to 20–25 m s^{-1} on the north side of the storm center, with a secondary wind maximum of 15–20 m s^{-1} located 170 km to the southeast. Although the Charlotte anemometer showed an isolated 1-min peak wind of 27 m s^{-1} that was simultaneous with the peak gust of 39 m s^{-1} at 0920 UTC, the trace (not shown) indicates cup anemometer overspeeding may have caused an inaccurate 1-min mean. The 10-min mean centered at this time was only 19 m s^{-1}. Compared with 0700 UTC, observations to the south of the center indicated that inflow increased in Hugo's wake on the southeast side, consistent with an acceleration in Hugo's forward motion.

In the aftermath, the public had a general impression that Hugo weakened very little between Charleston and Charlotte. Actually, based upon central pressure increases and mean wind speeds, Hugo weakened rapidly over that 6-h period. Hugo's MSLP increased from 934 mb with maximum mean winds of ~50 m s^{-1} at the coast near Bulls Bay to 970 mb and maximum mean winds of 20–25 m s^{-1} in only 6 h. This rate of decay,

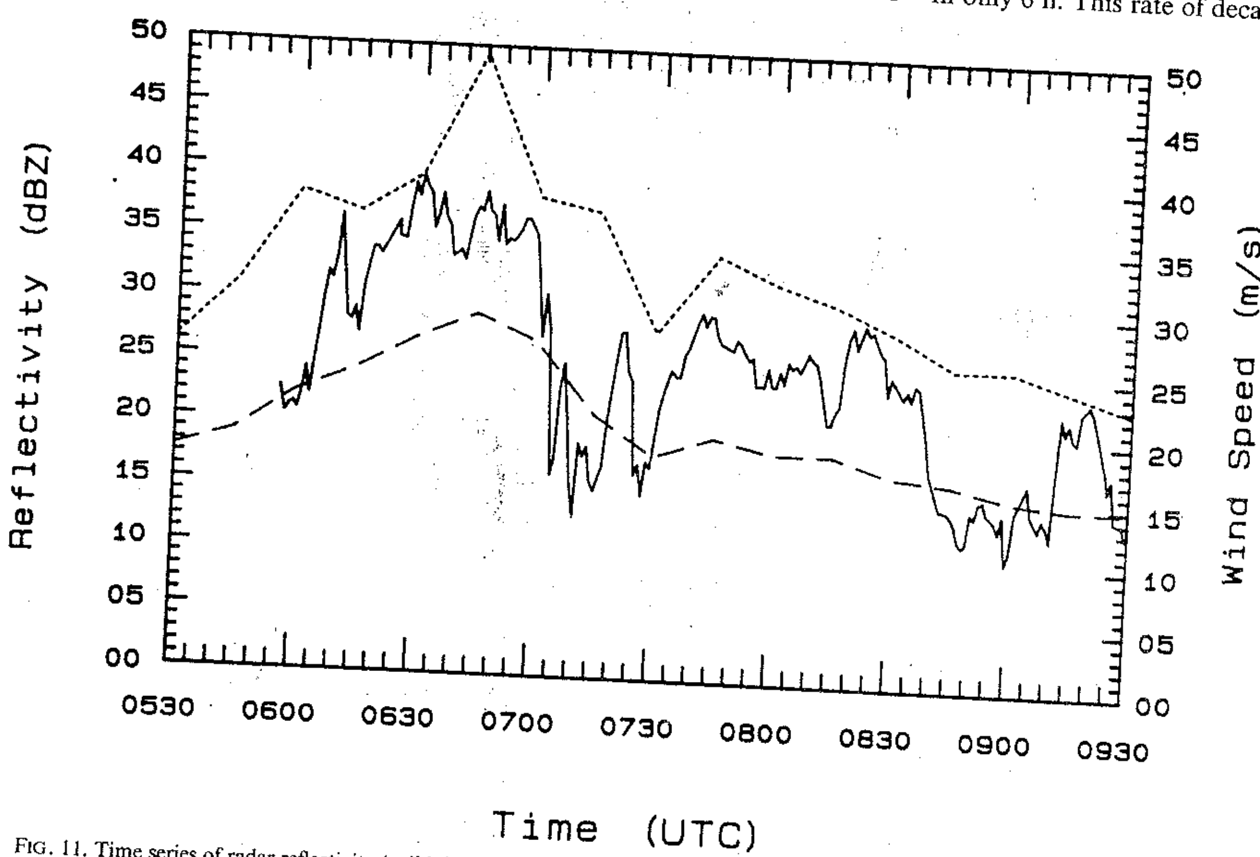

FIG. 11. Time series of radar reflectivity (solid line) for the location of Shaw Air Force Base as measured by the Charleston NWS radar. Peak gusts and 15-min mean winds (dashed lines) are from the Shaw Air Force Base anemometer trace from 0530–0930 UTC on 22 September 1989.

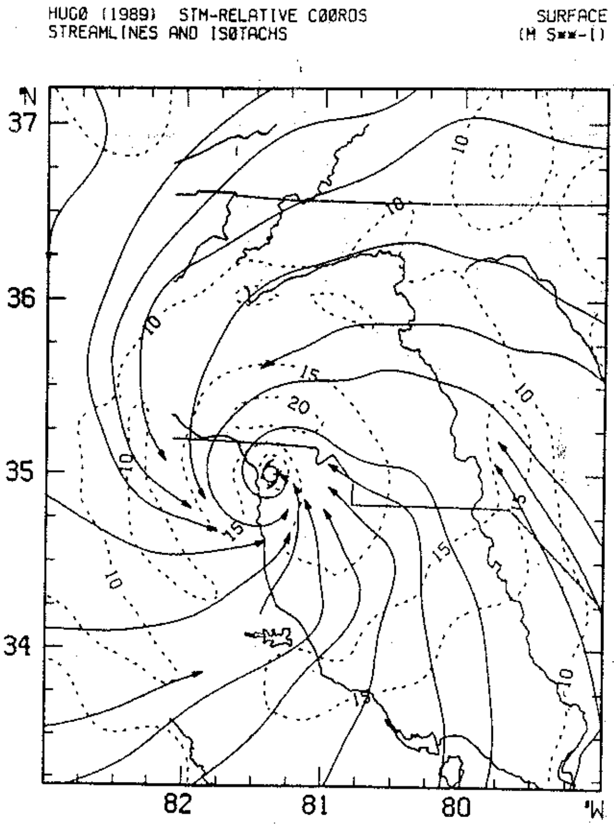

FIG. 12. As in Fig. 10, but for 1000 UTC on 22 September 1989 when Hugo was in the vicinity of Charlotte, North Carolina. Data collection input is 0800–1200 UTC.

~6 mb h^{-1}, is less than that for Hurricanes Hazel (1954, 11 mb h^{-1}) and Camille (1969, 8 mb h^{-1}), but larger than the average filling rate (~2 mb h^{-1}) of 11 hurricanes described by Malkin (1959).

6. Gust envelope and gust factors

Based upon postanalyses of the available mean wind observations, the NHC public advisories provided an accurate portrayal of Hugo's sustained winds after landfall. What the public may not have been prepared for, however, was the threat of wind gusts above hurricane force in northwest South Carolina and western North Carolina. Before 0400 UTC, wind gusts above hurricane force were forecast for a storm track through eastern South Carolina and North Carolina. At 0400 UTC, it became apparent that Hugo would track further to the west, and the advisory forecast was shifted, 6 h before Hugo reached Charlotte. The envelope of maximum gusts experienced by the observing sites during Hugo (Fig. 13) shows the dropoff with distance inland from 65 m s^{-1} at the southwest end of Bulls Bay to 36 m s^{-1} at Hickory, North Carolina (HKY in Fig. 1). Although mean winds subsided to below hurricane force by 0700 UTC, maximum gust speeds were above hurricane force as far north as HKY through 1046 UTC.

Gust speeds may be estimated by applying a gust factor to the mean wind of a given averaging period. The mean gust factor for offshore moored buoys from the comparison dataset of Powell and Black (1990b) indicates a ratio of 5–8-s gusts to 8.5-min mean winds of 1.3. Gust factors determined from digitized wind traces of land-based anemometers in Hurricanes Frederic, Alicia, Elena, and Hugo have recently been studied by Krayer and Marshall (1991). Based upon 265 segments of >18 m s^{-1} (10-min) mean winds and 2-s gusts adjusted to standard exposure (10-m height, roughness length of 0.03), Krayer and Marshall determined a mean gust factor of 1.5, consistent with values from overland sites (with 10–15-min mean winds) in Table 3. In locations that experienced extremely convective rainband features during eyewall passage in Hurricane Hugo, such as SSC, anemometer traces indicated that the 10-min gust factor could approach a value of 2.0. Very few buoy data show this tendency,

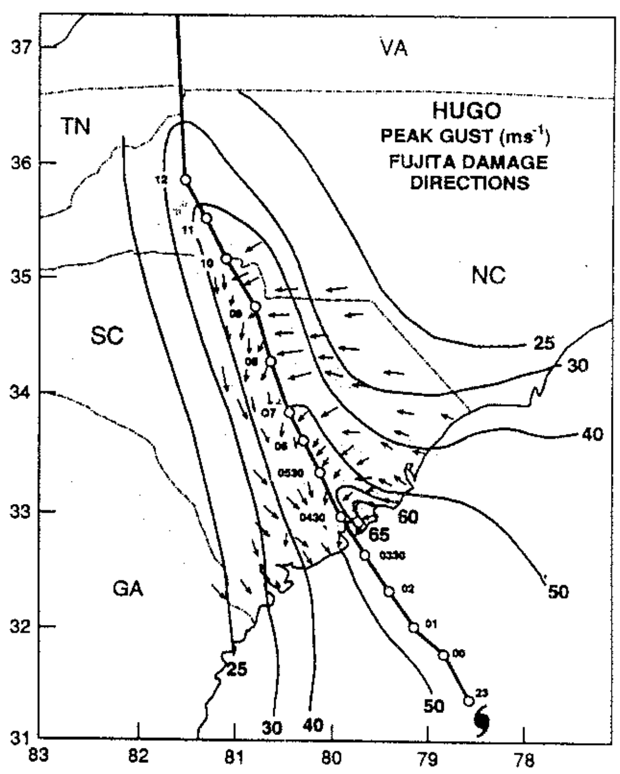

FIG. 13. Envelope of peak gusts relative to the track of Hugo's wind center. Superimposed are (first) damage vector directions as determined by aerial surveys supplied by Ted Fujita of the University of Chicago.

as evidenced by only 6 of 83 gust factors > 1.5 from a 1975–1990 set of aircraft-moored buoy comparisons. These results give us a good idea of how to estimate gusts from 8.5–10-min mean winds overland and offshore. For advisories however, the hurricane forecaster must estimate gusts from the V_{MSS}, a parameter that is not measured directly but is estimated from other measurements and the forecaster's experience.

The results above may be extended to estimate gust factors for the V_{MSS} by using wind statistics of Durst (1960) to relate extreme winds of various averaging periods. This method examines the relationship of the maximum 2-s, 1-min, and 10-min mean values measured over an hour to the hourly mean. Provided the Durst relationships are appropriate for hurricane conditions inland or offshore, over a period of an hour, the peak 1-min mean (V_{MSS}) is 15% larger than the peak 10-min mean and 11% larger than the peak 8.5-min mean measured by a buoy.

The method outlined by Krayer and Marshall (1991) converts gust factors to an hour reference period, after which the relationships of Durst may again be used to relate gusts to a V_{MSS} reference measurement. Krayer and Marshall's mean hurricane gust factor of 1.5 converts to a ratio of the peak 2-s gust to the V_{MSS} over an hour of 1.3. Based upon the mean offshore moored buoy gust factor, the ratio of the peak 5–8-s gust to the V_{MSS} offshore would be 1.15. In extreme convective conditions over land, a gust factor of 2.0 would convert to a ratio of the peak 2-s gust to the V_{MSS} of 1.65. Hence, offshore, the peak 2-s gust would be estimated at 15% larger than the V_{MSS}, and inland, the peak 2-s gust would generally be 30% larger than the V_{MSS} in all but the most extreme convective conditions, where it would be 65% larger. These ratios are summarized in Table 4 and imply that the V_{MSS} and peak gust occur over the same 60-min period.

We compared these values with ratios that were computed from the highest peak gusts and maximum sustained winds over the period of the storm; these were available from selected surface stations with continuous records and are presented in Table 5. The mean gust factor for the 12 stations was 1.52. Of the six stations affected by the eyewall (CHS, CUS, SSC, CAE, CLT, and HKY), only HKY and SSC show values >1.6. Of the next highest gust factors, NBC and SAV were associated with an outer rainband, but it is not known whether the large value at RDU was associated with an outer rainband or turbulence associated with complex topography.

TABLE 4. Gust factors to be used with maximum sustained surface winds (V_{MSS}).

Over-ocean and on-coast (oceanic exposure):	1.15 (use with over-water V_{MSS})
Overland and inland (airport exposure):	1.30 (use with V_{MSS} adjusted for decaying storm)
Extreme convection and complex terrain turbulence (eyewall, rainbands, hills):	1.65 (use with V_{MSS} adjusted for decaying storm)

TABLE 5. Ratios of storm-maximum peak gusts to the maximum surface sustained (1-min average) winds measured during Hugo at selected stations.

Station ID	Time (UTC) ($m\ s^{-1}$)	Peak gust ($m\ s^{-1}$)	V_{MSS}	Gust/V_{MSS}
Customs House (CUS)	0340	48.5	35.0	1.38
Charleston (CHS)	0503	43.8	39.1	1.12
Florence (FLO)	0547	27.8	20.1	1.38
Savannah (SAV)	0553	24.2	15.5	1.56
Myrtle Beach (MYB)	0555	34.0	23.2	1.46
Columbia (CAE)	0609	31.4	23.7	1.32
Shaw AFB (SSC)	0655	49.0	29.8	1.64
Beaufort (NBC)	0700	22.6	13.9	1.63
Charlotte (CLT)	1003	39.1	30.9	1.26
Hickory (HKY)	1046	36.1	15.5	2.37
Raleigh (RDU)	1050	23.7	12.8	1.85
Greensboro (GSO)	1108	24.2	19.1	1.27
			Mean	1.52
			σ	±0.33

Note that the relationships between the 1-h mean and the maximum 10-min and 1-min winds over that hour are based upon Durst's results from a few episodes of several hours of data collected over land in non-tropical cyclone conditions. A similar study was undertaken by Bell (1961) for Hong Kong typhoons, but the results may have been affected by the proximity of island topography upwind of the anemometer. Deacon's (1965) results for overland flow over level terrain in Victoria, Australia, were very similar to Durst's, but mean winds were <19 m s^{-1}. Clearly, many additional time series type data are needed to validate these conversion methods for both overland and marine exposures in hurricane conditions. Once the forecaster is confident of the V_{MSS} value determined for his advisory, offshore and coastal gusts can be estimated as 15% higher. For stations inland from the coast, frictional effects decrease the V_{MSS} that a particular station might measure, but increase the gust factor. Advisories issued subsequent to landfall should address this fact by adjusting the V_{MSS} downward and by estimating peak gusts as 30% higher than this value, except in extreme convection in the eyewall and rainbands where gusts would be 65% higher. More detailed examination of moored buoy data in hurricanes is necessary to determine the magnitude of gust factors related to extreme convection in the eyewall offshore.

7. Fujita's damage direction analysis

Included in Fig. 13 are directions of "first" damage (the debris closest to the surface) determined by Professor T. Fujita (personal communication, 1990) in an extensive aerial survey of damage patterns. These patterns indicate areas where swaths of extreme winds contributed substantial damage in small areas aligned with the wind. These swaths are probably associated with the extreme-type gust factors mentioned above. Fujita has extensively analyzed these regions in Hugo and earlier hurricanes. He believes that they were due to "downbursts" that were caused by strong downdrafts spreading out at the ground from convective cells in rainbands. Fujita found no clear evidence of tornadoes in his analysis. We overlayed wind analyses on the track at various times and noted locations where damage and wind directions coincided to discern the time period of the damage. Damage directions were then compared with radar reflectivity analyses during these periods, which suggested that nearly all the damage directions were associated with the eyewall wind maximum.

8. Conclusions and recommendations

Uncertainty in the distribution of the surface wind field, and in forecast track, storm intensity, and evacuation lead time, contribute to large hurricane warning areas and high preparedness costs. A real-time surface wind analysis system capable of using high-resolution aircraft in situ and remotely sensed measurements, with conventional observations from offshore and coastal platforms, has the potential to reduce uncertainty in the surface wind field. The analysis method for this system (Ooyama 1987) was applied to a landfalling hurricane for the first time to help document the surface wind distribution of Hurricane Hugo. Advantages of the method include a user-selectable scale control, which allows filtering of observational noise on scales unresolved by the data. The result is an analysis that is representative of the scales of interest. In analysis of surface wind fields, this degree of accuracy is especially important because of large variability in sampling methods, instrument heights, exposure, and fetch, and the presence of small-scale circulations and turbulence that cannot be fully resolved by the data.

Hurricane wind strengths are defined on the basis of the V_{MSS}, a parameter that is not routinely measured, with a spatial scale on the order of convective fluctuations that cannot be resolved by the observations. The goal of the analysis system is to provide the forecaster with sufficient high-quality mesoscale information to accurately estimate the V_{MSS} and extent of the wind field. The analysis wind fields are roughly equivalent to 13–20-min averages and resolve the important mesoscale features of the hurricane circulation: the eyewall and rainband wind maxima. High-resolution time series data in hurricanes will be required to determine the relationship of longer-time-period average winds to the V_{MSS}.

Analyses of Hugo's wind field were performed in a storm-relative system over three time windows of several hours; they are representative of the mean condition of the decaying storm over each period. At landfall, Hurricane Hugo's maximum surface winds were confined to a small region in the north to northeast portion of the eyewall. These winds reached 50 m s^{-1} in the coastal area of Bulls Bay in South Carolina, with gusts to 66 m s^{-1}. Just inland, winds decreased considerably because of frictional effects within a few kilometers of the coast. Wind profiles from airborne Doppler radar over water and a rawinsonde over land indicate maximum wind levels between 0.5- and 2-km heights and very strong wind shear over land.

By 0700 UTC, 3 h after landfall, Hugo's maximum surface winds decreased to just below hurricane force (30 m s^{-1}) in the vicinity of Columbia and Sumter, South Carolina. Despite the decay of Hugo's mean circulation to below hurricane force by 0700 UTC, surface wind gusts exceeded hurricane force in locations near the eyewall until 1000 UTC. Six hours after landfall, Hugo reached the Charlotte, North Carolina, area with tropical-storm-force winds (19 m s^{-1}) and gusts to 39 m s^{-1}. In an effort to improve estimation of surface gusts for use in advisories, mean hurricane gust factors for moored buoys (8.5-min average) and overland anemometers (10-min average) were converted to 1-min gust factors following the methods of Krayer and Marshall (1991) and Durst (1960). These factors may be added to the V_{MSS} to estimate wind gusts; 15% offshore and at the coast, 30% inland (with reduced V_{MSS}), and 65% inland (also with reduced V_{MSS}) in extremely convective portions of the eyewall and major rainbands. At present, it does not appear that extreme gust factors ($\geq$2.0) are prevalent in eyewall passages over moored buoys. Improved warnings of the potential for gust damage could be achieved by incorporating these estimates in the marine advisories before landfall and in the public advisories subsequent to landfall.

Determination of the surface wind field in Hugo at landfall was hampered by a lack of data in the part of the storm where aircraft had measured maximum flight-level wind speeds. Fortunately, there were enough surface observations in other portions of the storm to allow empirical adjustment of the aircraft measurements. Empirical adjustment of flight-level winds assumes that the level of maximum wind speed coincides with the aircraft altitude; an assumption that may be valid only in an upright eyewall. This approach will be unnecessary if remote sensing of surface wind speeds becomes a feature on reconnaissance aircraft. The stepped frequency microwave radiometer (SFMR) (Black and Swift 1984; Tanner et al. 1987) has shown great promise. The prototype SFMR has performed well in extensive tests by HRD over the past several hurricane seasons on the NOAA aircraft. In 1991, the SFMR measurements will be sent to NHC in real time via ASDL. The 44th Interdepartmental Hurricane Conference (Carnahan 1990) recommended that NOAA and the U.S. Air Force procure SFMRs for all reconnaissance aircraft.

To improve specification of the surface wind field in hurricanes, expansion of the CMAN, moored-buoy, and automatic surface observation network is desired. CMAN and moored-buoy observations have been invaluable for marine forecasting and for studying oceanic wind fields in hurricanes. The 45th Interdepartmental Hurricane Conference (Carnahan 1991) recently endorsed a sampling strategy for automatic surface stations (Appendix) that should greatly improve surface wind field specification. Additional observations could be gathered through support of a program (Appendix) through which universities could receive support to site one or more automatic wind stations in advance of a landfalling hurricane. This would avoid logistical problems involved with sending outside investigation teams into unfamiliar areas. Installation of well-exposed wind sensors at amateur radio network locations (Appendix) would greatly assist documentation of hurricane landfalls in remote areas of developing countries.

Acknowledgments. One of the authors (MDP) would like to thank the National Research Council Committee on Natural Disasters for the opportunity to serve as a member of the Hugo disaster study team for the landfall in the Carolinas. This investigation could not have been attempted without the cooperation of many individuals in helping to supply needed data. Especially important are those who assisted during a period of great personal and professional stress during poststorm recovery operations. We wish to acknowledge the assistance of Richard Shenot and staff of the NWS in Charleston, Albert Hinn and the NWS staff in Wilmington, Peter Sparks of Clemson University, Miles Lawrence of NHC, Ted Fujita of the University of Chicago, Peter Black, Frank Marks, Mark DeMaria, Sim Aberson, Paul Leighton, Mike Shoemaker, Bob Wright, and Bill Barry of HRD, Stephen Baig of NESS, and Richard Marshall of NIST. The editorial assistance of Constance Arnhols, manuscript processing by Gail Derr, graphics by Dave Senn, and photography by Andy Ramsay are also acknowledged. Constructive comments on an earlier version of the manuscript by James Franklin, Bob Sheets, and one anonymous reviewer were appreciated.

APPENDIX

Surface Wind Sampling Considerations and Analyses in Hurricanes

a. Observation averaging time

A serious problem affecting surface wind analysis concerns lack of standardization of averaging times. In the United States, the NWS standard for averaging time of surface wind observations is to report the 1-min average wind (also known as the sustained wind). NOAA Data Buoy Center marine observations consist of a 2-min average for CMAN stations and an 8.5-min average for moored buoys. The standard wind speed averaging time recommended by the WMO of the United Nations is 10 min. The 10-min observation has been shown (Pierson 1983) to give a much better estimate of the mesoscale wind features that must be resolved for forecast improvements. In hurricane conditions, as shown by the anemometer trace from Charleston (Fig. 14), a 1-min observation does not give a stable estimate of the wind speed compared with a 10-min value.

The nonrepresentativeness of short-period means depends upon the spatial scales of the wind features measured. Representative sampling volumes measured by various anemometer platforms used in this study were estimated by computing the length of an air volume sampled by a platform over the averaging time period. These lengths are plotted against averaging time on logarithmic scales as a function of wind speed in Fig. 15. According to Fig. 15, stationary platform averages of 1 min are associated with microscale and convective-scale wind features that are highly variable and cannot be resolved or predicted, while 10-min means correspond to the mesoscale features that we wish to resolve and forecast.

b. Conversion of mesoscale analyses to V_{MSS}

Unfortunately, it is impossible to correct or convert averaging times to a particular sampling period. Methods (e.g., Durst 1960) are available for estimating the peak short-period wind speed within a longer-period wind average. For example, from a 1-h average, it would be possible to estimate the peak 1-min or peak 10-min wind within the 60-min period. However, there is no method for converting a 10-min mean wind observation taken on the hour to a 1-min mean or vice versa. Rather than trying to convert all analysis input data to a common averaging time, a more feasible approach for surface analyses would be to assimilate all the types of surface data into the objective analysis scheme with a user-selected scale control (such as Ooyama 1987) and with observations weighted according to relative accuracy. The analysis wind speed and filter scale could then be used to estimate a time scale for the analysis wind, based upon Fig. 15. Finally, the peak 1-min wind that could be expected to occur over that time scale could be computed using Durst's methods, assuming a stationary wind field with a normal distribution. The resulting analysis would still resolve important mesoscale details of the wind field (the

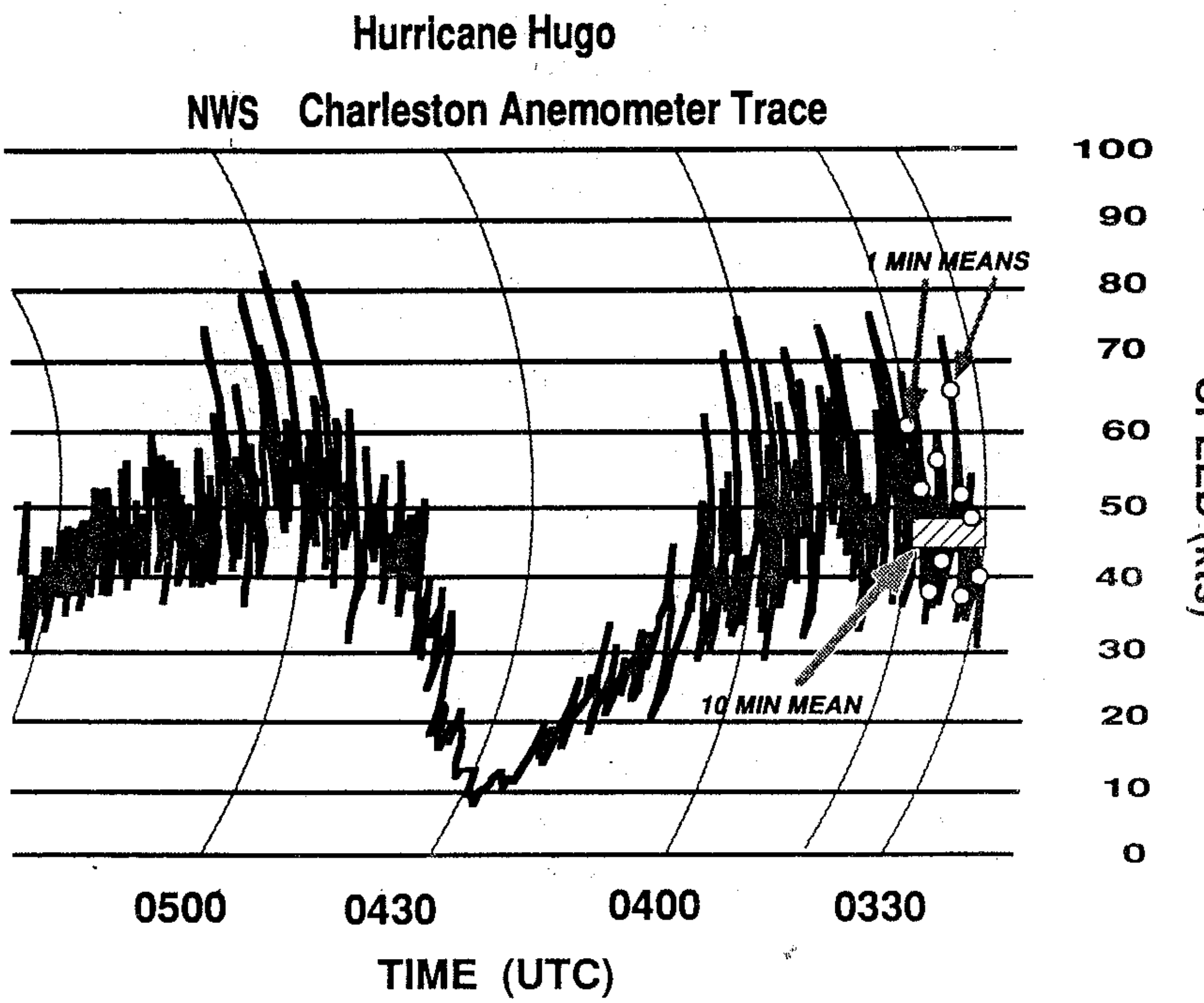

FIG. 14. Reconstructed anemometer trace from the Charleston NWS office indicating difference between 1-min averages and relative stability of 10-min average. Speeds are in knots.

eyewall and major rainbands) while providing forecasters with an estimate of the maximum sustained surface wind speed at any location within the analysis domain.

c. Automatic weather stations

As automatic surface weather observation stations begin to supplant manual sites, it is important to attempt to standardize surface observations to a common level and sampling strategy. With this in mind, the 45th Interdepartmental Hurricane Conference endorsed the following sampling strategy for automatic observing stations to serve the interests of the hurricane operations and research community:

1) Adopt WMO 10-min average at 10-m level for hourly observations.

2) Record consecutive 1-min means from 5-s block averages and permanently archive those data with the National Climatic Data Center.

3) Send peak 1-min and peak 5-s averages during the past hour with hourly observation.

4) Have the ability to interrogate a 10-min mean, peak 1-min average, and peak 5-s average, every 10 min under specified criteria.

d. Solutions for the problem of sparse wind observations

Clearly, higher-resolution measurements are required to correctly resolve the wind field of a hurricane, particularly in rural areas such as Bulls Bay. Apart from an expanded CMAN and automatic station network, there have been suggestions to set up an array of quickly

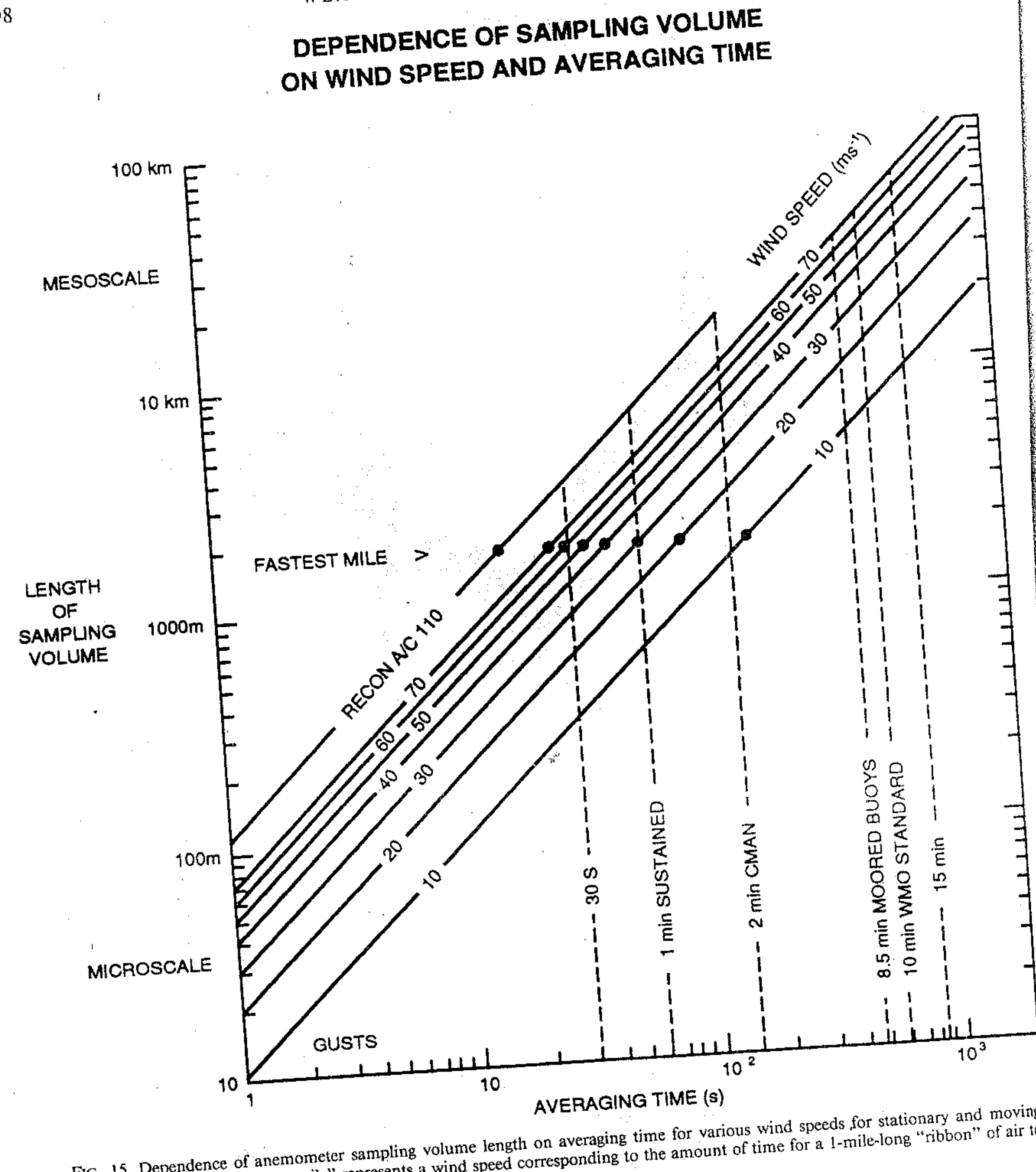

FIG. 15. Dependence of anemometer sampling volume length on averaging time for various wind speeds for stationary and moving (aircraft) platforms. The "fastest mile" represents a wind speed corresponding to the amount of time for a 1-mile-long "ribbon" of air to pass an anemometer.

deployable anemometers shortly before landfall. The logistical problems in this type of program are immense. Such instrumentation would have to be properly exposed at a reasonable height and guyed for stability with backup power. Installation of a wind observing site is no trivial matter. Anything that is quickly deployable is also quickly destroyable. To safely and properly set up instrumentation would require highly trained personnel to begin 36–24 h before projected landfall and site instruments over a large enough portion of the coastline to account for possible forecast errors.

Since the mean landfall point error at 24 h is near 90 km, a portion of the coast twice this distance would have to be instrumented at a spacing of 15–20 km to resolve the region of maximum winds. Hence, 12 sites and several installation teams would be required. The equipment would have to be centrally sited and trucked into the investigation area. Trained installation teams, flown in from outside, would have to rendezvous with the equipment and deploy it. Access to coastal locations in a timely fashion would have to be gained when advance evacuations have already begun and when NWS and other public officials are concerned with making emergency preparations. These concerns would make it highly unlikely that any local individuals with public service responsibilities would be able to assist in siting the instruments. Such a program could probably succeed, but would require several years and great expense for the proper documentation of one severe hurricane.

A better alternative would be to support selected universities along the coast with meteorology and/or civil engineering programs to develop plans to site one or more self-built instruments in a local hurricane episode. Local universities familiar with the area could preselect sites and acquire advance permission and clearances to deploy equipment, thereby avoiding many of the logistical problems and costs involved in using outside teams. This plan was successfully implemented by the Coastal Engineering Department of the University of Florida in Hurricanes Frederic and David in 1979.

An alternative that would especially benefit developing nations would be to instrument selected sites that participate in emergency communication operations as a part of the United Nations Amateur Radio Readiness Group (personal communication, David Rosen, associate director). Many of these sites already have guyed towers of 10-m height or more, with backup power. Anemometers could be installed at these sites, with proper site documentation and interfaced with a PC for archival.

REFERENCES

Arya, S. P., 1988: *Introduction to Micrometeorology.* Academic Press, 307 pp.

Bell, G. J., 1961: Surface winds in Hong Kong typhoons. Royal Meteorological Observatory, Hong Kong.

Black, P. G., and C. T. Swift, 1984: Airborne stepped-frequency microwave radiometer measurements of rainfall rate and surface windspeed in hurricanes. Preprints: *22nd Conf. Radar Meteorology,* Zurich, Switzerland, Amer. Meteor. Soc., 433–438.

Carnahan, R. L., 1990: Minutes of the *44th Interdepartmental Hurricane Conf.,* Homestead Air Force Base, Florida, Office of Fed. Coord. for Meteor. Services and Supporting Research, NOAA, Washington, D.C.

——, 1991: Minutes of the *45th Interdepartmental Hurricane Conf.,* Homestead Air Force Base, Florida, Office of Fed. Coord. for Meteor. Services and Supporting Research, NOAA, Washington, D.C.

Case, B., and M. Mayfield, 1990: The Atlantic hurricane season of 1989. *Mon. Wea. Rev.,* **118,** 1165–1177.

Deacon, E. L., 1965: Wind gust speed: Averaging time relationship. *Aust. Meteor. Mag.,* **52,** 11–14.

Durst, C. S., 1960: Wind speeds over short periods of time. *Meteor. Mag.,* **89,** 181–186.

Gilhousen, D. B., 1987: A field evaluation of NDBC moored buoy winds. *J. Atmos. Ocean. Tech.,* **4,** 94–104.

Jorgensen, D. P., 1984: Mesoscale and convective-scale characteristics of mature hurricanes. Part I: General observations by research aircraft. *J. Atmos. Sci.,* **41,** 1268–1285.

——, P. H. Hildebrand and C. L. Frush, 1983: Feasibility test of an airborne pulse-Doppler meteorological radar. *J. Atmos. Sci.,* **22,** 744–757.

Krayer, W. R., and R. D. Marshall, 1991: Gust factors applied to hurricane winds. Preprints: *Eighth International Conf. Wind Engineering,* London, Ontario, Canada, Int. Assoc. for Wind Engineering.

Liu, W. T., K. B. Katsaros and J. A. Businger, 1979: Bulk parameterization of air–sea exchanges of heat and water vapor including the molecular constraints at the interface. *J. Atmos. Sci.,* **36,** 1722–1735.

Lord, S. J., and J. L. Franklin, 1987: The environment of Hurricane Debby (1982). Part I: Winds. *Mon. Wea. Rev.,* **115,** 2760–2780.

Malkin, W., 1959: Filling and intensity changes in hurricanes over land. NHRP Rep. No. 34, U.S. Dept. Commerce, 18 pp. [Available from: NOAA/HRD, 4301 Rickenbacker Cswy, Miami, FL 33149].

Office of the Federal Coordinator for Meteorological Services and Supporting Research, 1990: National Plan for Tropical Cyclone Research. FCM-P25, Washington, D.C.

Ooyama, K. V., 1987: Scale-controlled objective analysis. *Mon. Wea. Rev.,* **115,** 2479–2506.

Panofsky, H. A., and G. W. Brier, 1965: *Some Applications of Statistics to Meteorology.* College of Mineral Industries, The Pennsylvania State University.

——, and J. A. Dutton, 1984: *Atmospheric Turbulence.* Wiley Interscience, 397 pp.

Parrish, J. R., R. W. Burpee, F. D. Marks and R. Grebe, 1982: Rainfall patterns observed by digitized radar during the landfall of Hurricane Frederic (1979). *Mon. Wea. Rev.,* **110,** 1933–1944.

Peterson, E. W., 1969: Modification of mean flow and turbulent energy by a change in surface roughness under conditions of neutral stability. *Quart. J. Roy. Meteor. Soc.,* **95,** 561–575.

Pierson, W. J., 1983: The measurement of the synoptic-scale wind over the ocean. *J. Geophys. Res.,* **88,** 1683–1708.

Powell, M. D., 1980: Evaluations of diagnostic marine boundary layer models applied to hurricanes. *Mon. Wea. Rev.,* **108,** 757–766.

——, 1982: The transition of the Hurricane Frederic boundary layer wind field from the open Gulf of Mexico to landfall. *Mon. Wea. Rev.,* **110,** 1912–1932.

——, 1987: Changes in the low-level kinematic and thermodynamic structure of Hurricane Alicia (1983) at landfall. *Mon. Wea. Rev.,* **115,** 75–99.

——, and P. G. Black, 1990a: Meteorological aspects of Hurricane Hugo's landfall in the Carolinas. *Shore and Beach,* **58,** 3–14.

——, and ——, 1990b: The relationship of hurricane reconnaissance flight-level wind measurements to winds measured by NOAA's oceanic platforms. *J. Wind Eng. Indust. Aerodynam.,* 36, 381–392.

SethuRaman, S., 1979: Atmospheric turbulence and storm surge due to Hurricane Belle (1976). *Mon. Wea. Rev.,* **107,** 314–321.

Sheets, R. C., 1990: The National Hurricane Center—Past, present, and future. *Wea. Forecasting,* **5,** 185–232.

Tanner, A., C. T. Swift and P. G. Black, 1987: Operational airborne remote sensing of windspeeds in hurricanes. Preprints: *17th Conf. Hurricanes and Tropical Meteorology,* Miami, Amer. Meteor. Soc., 385–387.